Gamma-ray emission from young radio galaxies and quasars

Principe Giacomo*[1,2,3],

L. Di Venere[4,5], M. Orienti[3], G. Migliori[3], F. D'Ammando[3],

on behalf of the Fermi-LAT collaboration,

[1]Dipartimento di Fisica, Università di Trieste, Trieste, Italy
[2]Istituto Nazionale di Fisica Nucleare, Trieste, Italy
[3]INAF - Istituto di Radioastronomia, Bologna, Italy
[4]Dipartimento di Fisica, Università e Politecnico di Bari, Bari, Italy
[5]Istituto Nazionale di Fisica Nucleare, Bari, Italy

Content

1. **Introduction: gamma-ray expectations for young radio sources**
2. **Sample of young radio sources**
3. **Fermi-LAT: data selection and analysis description**
4. **Fermi-LAT results:**
   - **individual sources**
   - **stacking analysis**
5. **Discussion**
   Investigating the origin of the gamma-ray emission
6. **Conclusion**

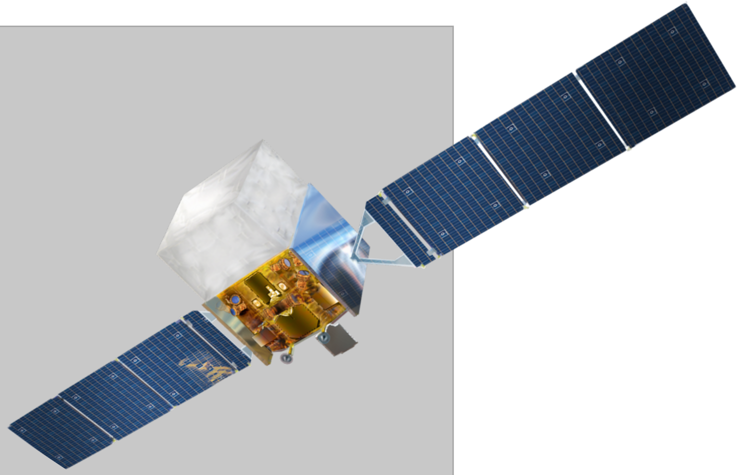

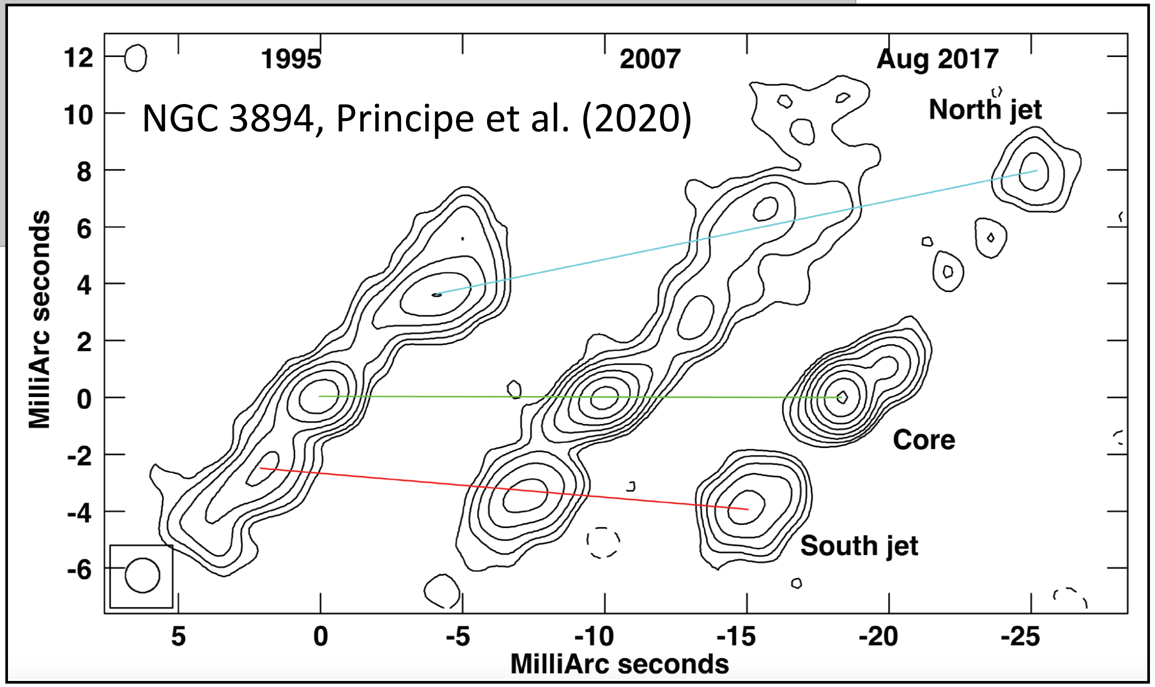

Gamma-ray expectation for young radio sources

Gamma-ray sky dominated by blazars. Only 2% are radio galaxies (or misaligned AGN), larger jet inclination angles (>10°) and smaller Doppler factor δ≤2−3 (*4LAC*, Fermi-LAT coll. 2019)

Evolutionary scenario (*Fanti et al. 1995; Readhead et al. 1996; Snellen et al. 2000*):

- the size of a radio source is strictly related to its age,
- given their intrinsically compact size, the population of GHz-peaked spectrum (GPS, size<1kpc) and compact steep-spectrum (CSS, size>1kpc) radio sources were proposed as the progenitors of classical radio galaxies.

Gamma-ray emission is expected: mainly due to Inverse Compton of the UV photons from the disk upscattered by the lobes' electrons [*Stawarz et. al. (2008)*].

The high-energy luminosity strictly depends on: linear size, jet power, UV photons, energy range, equipartition condition

$$\frac{\epsilon L_\epsilon}{10^{42}\mathrm{erg/s}} \sim 2\frac{\eta_e}{\eta_B}\left(\frac{L_{\mathrm{jet}}}{10^{45}\mathrm{erg/s}}\right)^{0.5}\left(\frac{LS}{100\mathrm{pc}}\right)^{-1}\frac{L_{UV}}{10^{46}\mathrm{erg/s}}\left(\frac{\epsilon}{1\mathrm{Gev}}\right)^{-0.25}$$

$$\frac{(\epsilon S_\epsilon)_{\mathrm{IC/UV}}}{10^{-12}\ \mathrm{erg\ cm^{-2}\ s^{-1}}} \sim 1.6\left[\frac{(\epsilon L_\epsilon)_{\mathrm{IC/UV}}}{10^{42}\ \mathrm{erg\ s^{-1}}}\right]\left(\frac{d_L}{100\ \mathrm{Mpc}}\right)^{-2}$$

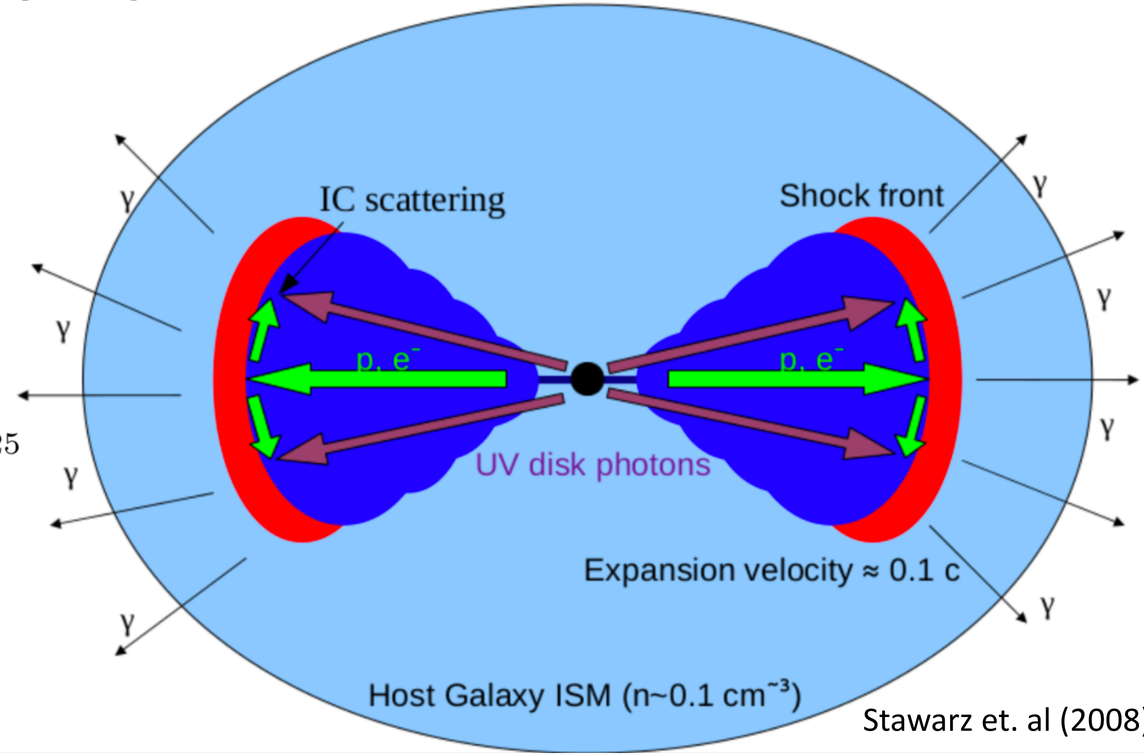

Stawarz et. al (2008)

So far ...

Systematic searches for young radio sources in gamma-rays have so far been unsuccessful (D'Ammando et al. 2016), while dedicated studies have reported a handful of detections: the young radio galaxies **NGC 6328** (a.k.a. PKS 1718-649, Migliori et al., 2016) and **NGC 3894** (Principe et al., 2020). The 4FGL source **TXS 0128+554** (BCU*, in 4FGL-DR2) has been recently reclassified as young radio galaxy by Lister et al. (2020).

NGC 3894 (Principe et al. 2020)
est. age: 58 $\pm$ 5 years, (LS~4 pc)
viewing angle: 10°< θ< 21°, δ~1.6

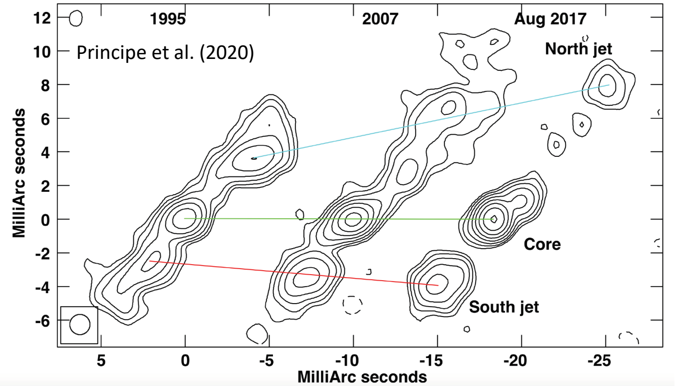

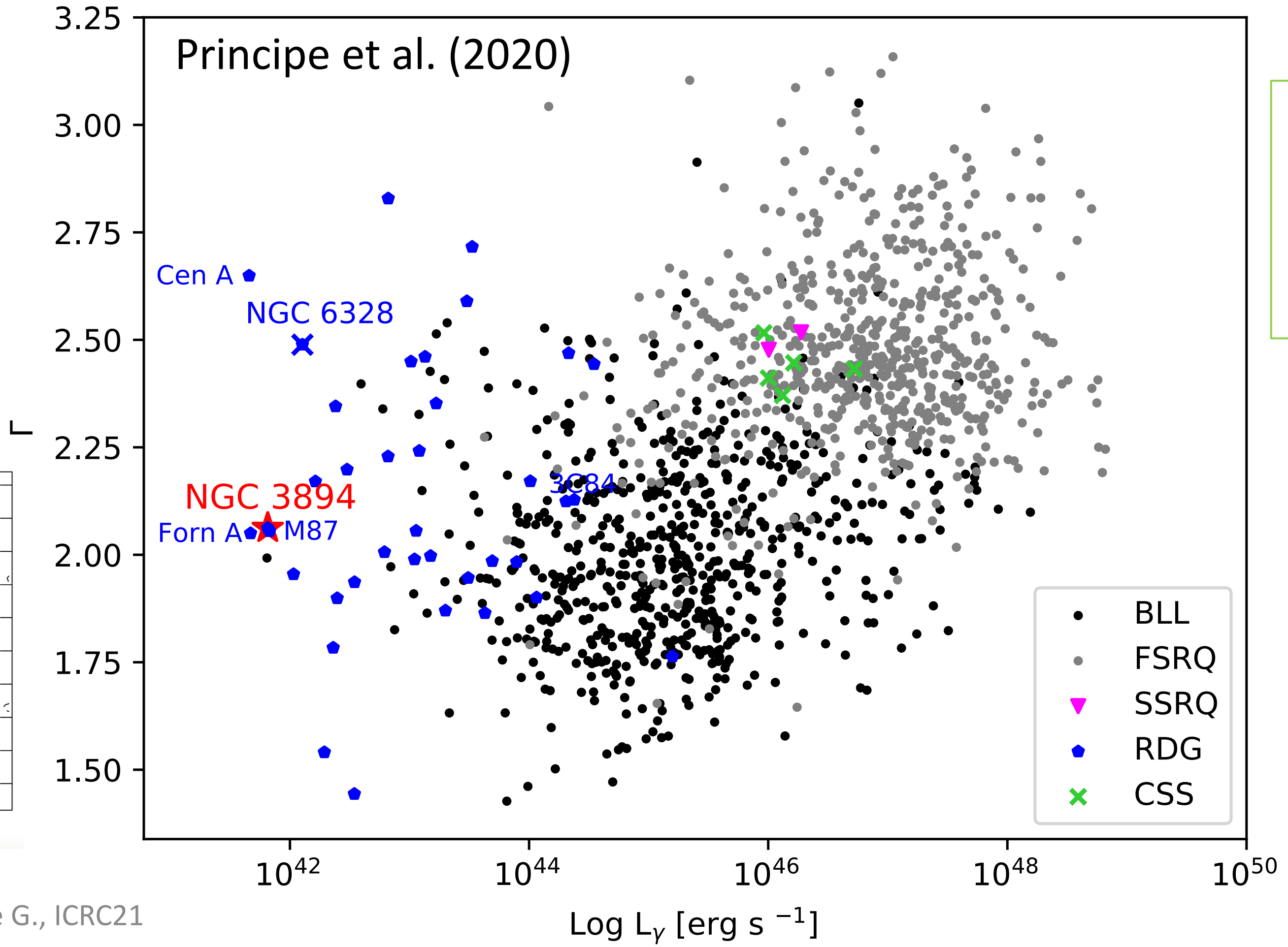

*BCU: blazar candidate of unknown type

4FGL contains also 6 CSS-quasars: 3C 138, 3C 216, 3C 286, 3C 309.1, 3C 380, PKS B1413+135; while quasar PKS 0056-00, first reported in 4FGL-DR2.

*Association of a 4FGL source to the (possible) young radio source **PMN J1603-4904.** However this source present a typical blazar emission with high gamma-ray variability.*

Sample of young radio sources

For this work we used 162 young radio sources (103 galaxies, 59 quasars), selected from the following resources:

- bona fide radio sources selected using VLBA observations by *Orienti & Dallacasa (2014) [51]*
- nearby (z<0.25) and compact (<2”) radio galaxies contained in the CORALZ sample (Snellen et al. 2004) [25]
- young radio AGNs selected based on SDSS spectroscopy by Liao & Gu (2020) [126]
- GPS and/or CSOs with measured redshifts below 1 and linear sizes below 1 kpc, realized by Wójtowicz et al. (2020), [29]

Final sample

Linear size (LS): 79 CSOs (LS < 1 kpc), 46 MSO (LS: 1 - 10 kpc), 37 sources 10 < LS < 50 kpc.

Radio turnover frequency (f_p): 52 GPS (f_p > 0.5 GHz), 110 CSS (f_p < 0.5 GHz).

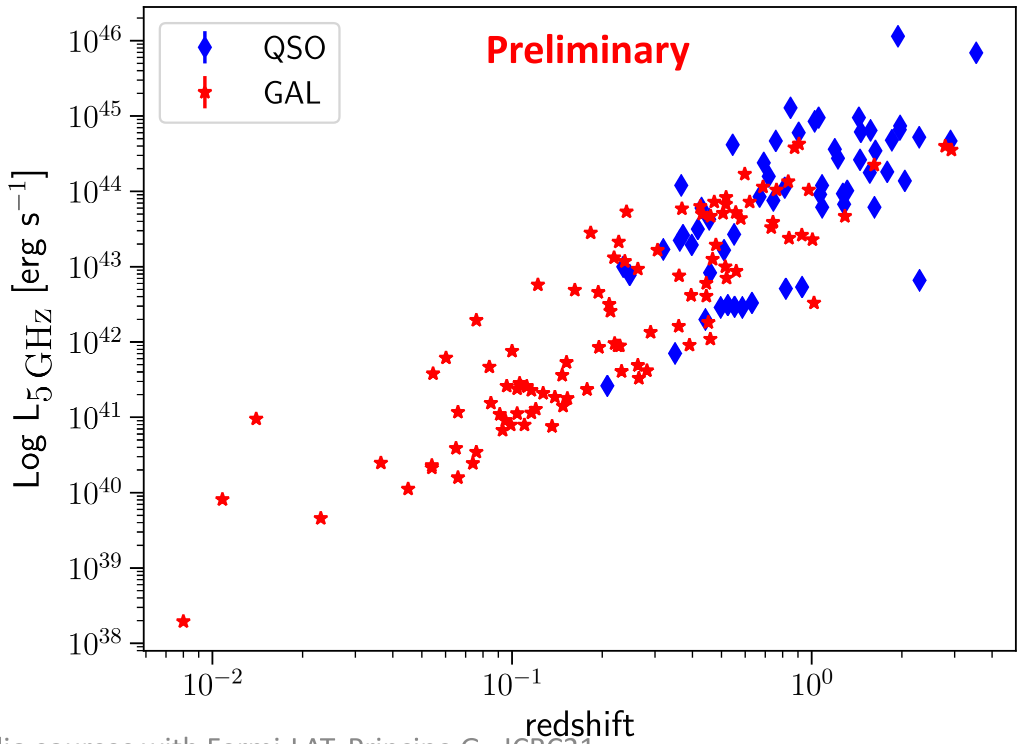

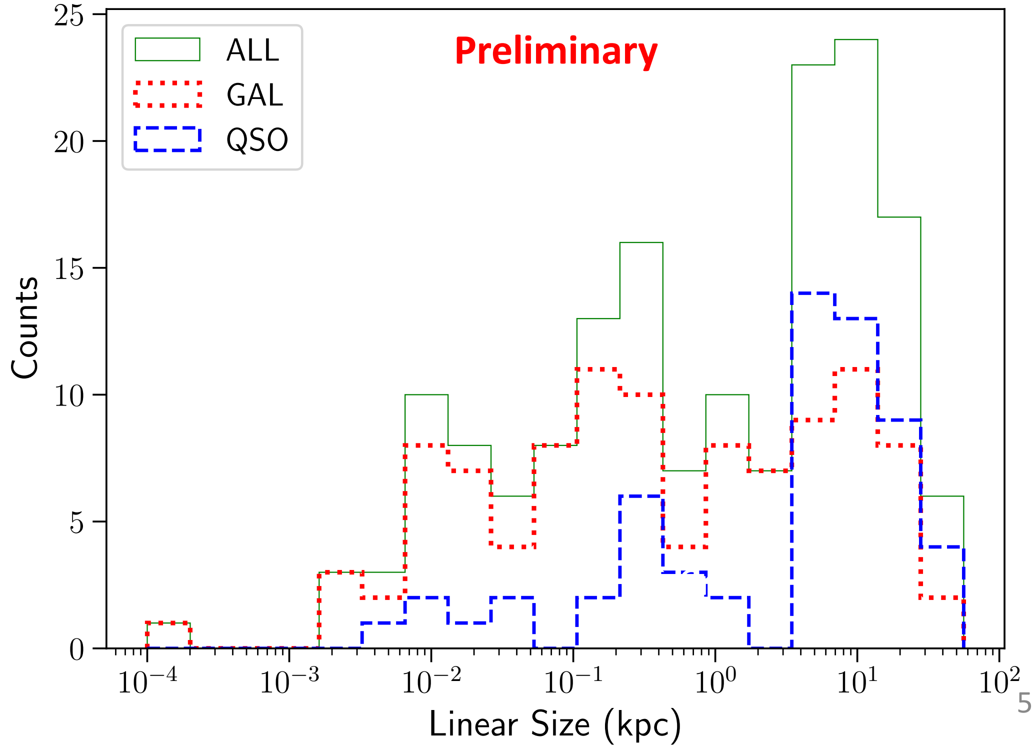

Analysis description

Analysis:
1. Likelihood analysis on each single source
optimization, fit, localization(TS>10),SED, lightcurve (1yr bin)
2. Stacked analysis on the undetected (TS<25) sources

We performed the analysis using Fermipy (v. 0.17.4)

Diffuse models:

- galdiff: gll_iem_v07.fits
- isodiff: iso_P8R3_SOURCE_V2_v1.txt

Model for the Fermi-LAT extend sources:

- LAT_extended_sources_8years.fits

Catalog:

We use one of the latest version of the **4FGL**:

- gll_psc_v21.fit

For a comparison of the results we also used the *4FGL-DR2*

Data Selection	Values
IRFs	P8R3_SOURCE_v2
PSF Classes	All [PSF0 and PSF1 excluded, E < 300 MeV] [PSF0 excluded, 300 MeV < E < 1 GeV]
Time Intervals	**11.3 years**
Energy Range	100 MeV – 1 TeV
Zenith angle	< 105° [< 85°, E < 300 MeV] [< 95°, 300 MeV < E < 1 GeV]
Pixel Size	0.1°

Results on single sources

In our analysis we detected 11 sources (4 galaxies and 7 quasars):

* we report the discovery of gamma-ray emission from a compact radio galaxy: PKS 1007+142.★

⁺ 5 quasars present significant gamma-ray variability.

	Name	type	z	LS kpc	ν_p GHz	log $L_{5\,GHz}$ W Hz^{-1}	TS	F_γ 10^{-9} cm^{-2} s^{-1}	Γ	L_γ 10^{44} erg s^{-1}	TS_{var}
	Galaxies										
GALAXIES	NGC 6328	CSO/GPS	0.014	0.002	4	24.28	36	5.30±1.45	2.60±0.14	0.011	5
GALAXIES	NGC 3894	CSO/GPS	0.0108	0.010	5	24.60	95	2.03±0.48	2.05±0.09	0.006	11
GALAXIES	TXS 0128+554	CSO/GPS	0.0365	0.012	0.66	23.69	178	8.03±1.46	2.20±0.07	0.19	9
GALAXIES	PKS 1007+142* ★	MSO/GPS	0.213	3.3	0.5-2	25.71	31	4.65±1.55	2.55±0.18	2.8	4
	Quasars										
QUASAR	3C 138†	MSO/CSS	0.759	5.9	0.176	27.97	34	2.09±0.89	2.05±0.12	64	68
QUASAR	3C 216†	LSO/CSS	0.6702	56	0.066	27.23	153	7.78±0.98	2.60±0.09	97	24
QUASAR	3C 286	LSO/CSS	0.85	25	<0.05	28.41	67	5.60±1.10	2.52±0.12	110	8
QUASAR	3C 309.1†	MSO/CSS	0.905	17	<0.076	28.08	207	6.33±0.74	2.47±0.07	180	215
QUASAR	3C 380†	MSO/CSS	0.692	11	<0.05	27.68	2274	36.44±1.48	2.41±0.03	510	68
QUASAR	PKS 0056-00	MSO/CSS	0.719	15	<0.14	27.50	52	5.21±1.48	2.30±0.15	74	11
QUASAR	PKS B1413+135†	CSO/GPS	0.247	0.03	8.4-15	26.19	1198	14.72±1.02	2.10±0.03	28	321

Results on single sources

Detected young radio sources are labeled in the plot

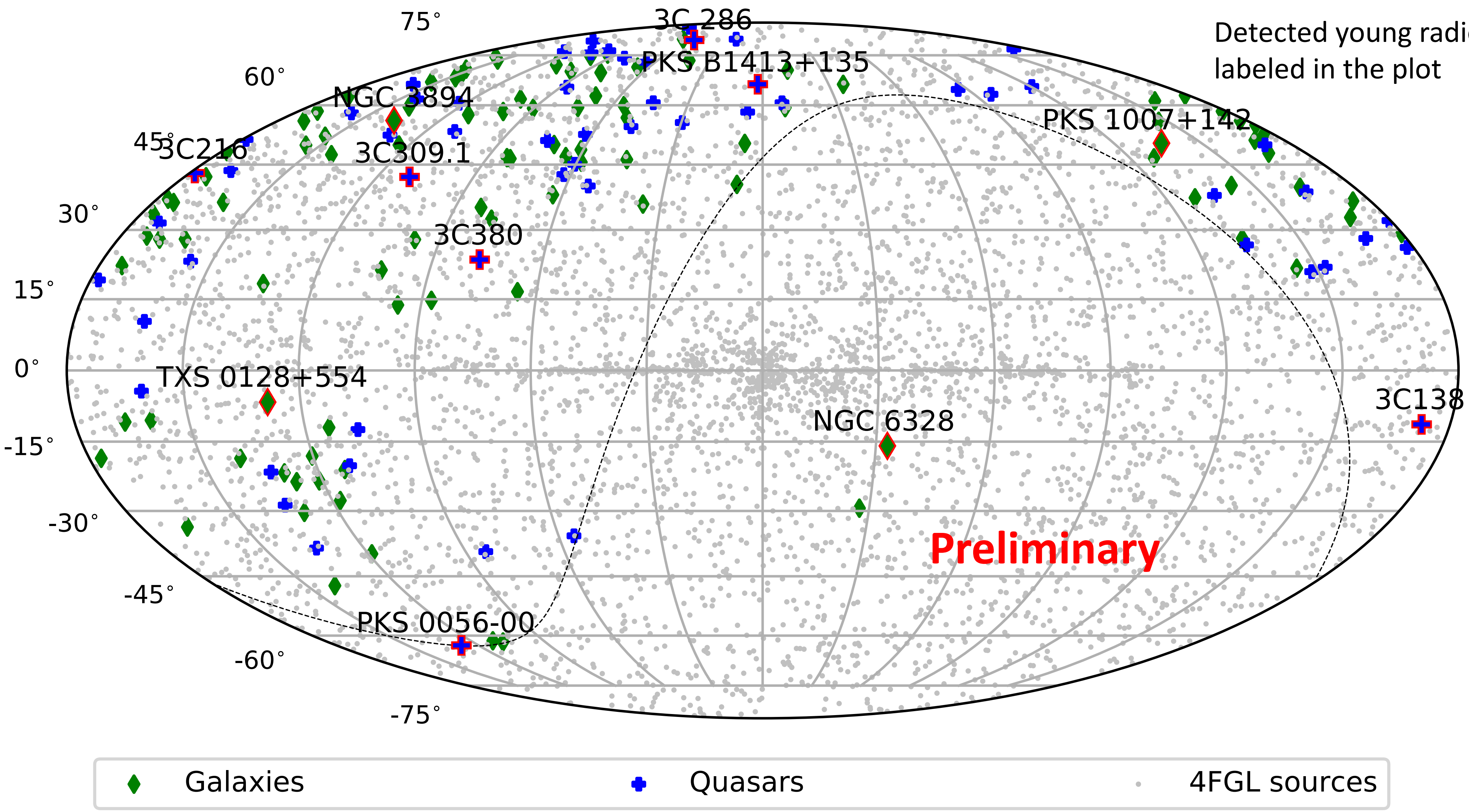

PKS 1007+142

PKS 1007+142 (MSO/GPS, z=0.213, LS=3.29 kpc)

Fermi results

Sign.: TS=31

Loc.: (R.A.,decl.(J2000)) = (152.43°± 0:07°, 14.08°± 0.06°) -> ass. prob. P=0.92

SED – PL: Γ= 2.55±0.18 , N_0=(1.72±0.39)x10^{-13} MeV cm^{-2} s^{-1}

Lightcurve: No significant gamma-ray variability observed (TS_{var}= 8)

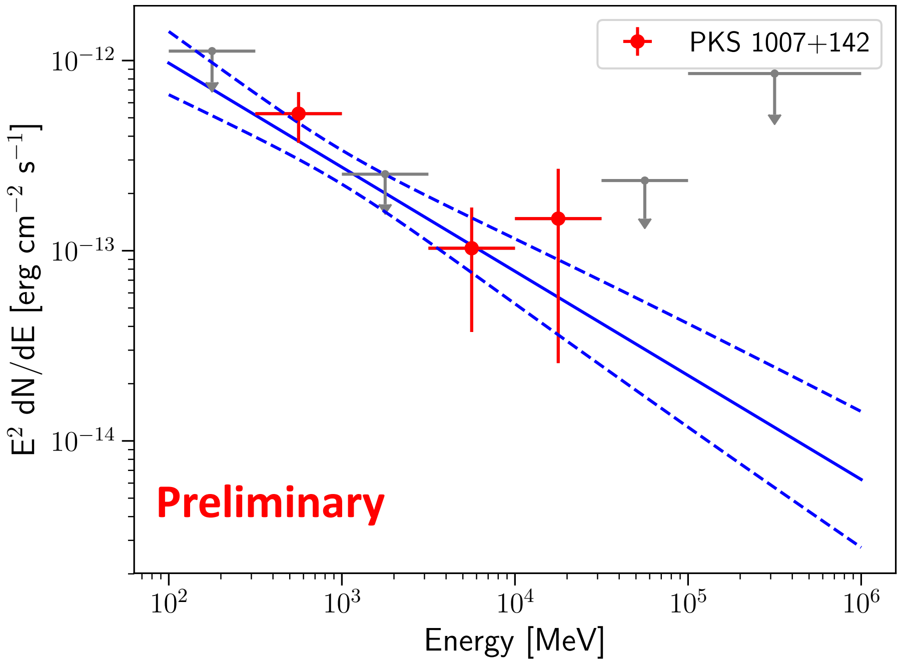

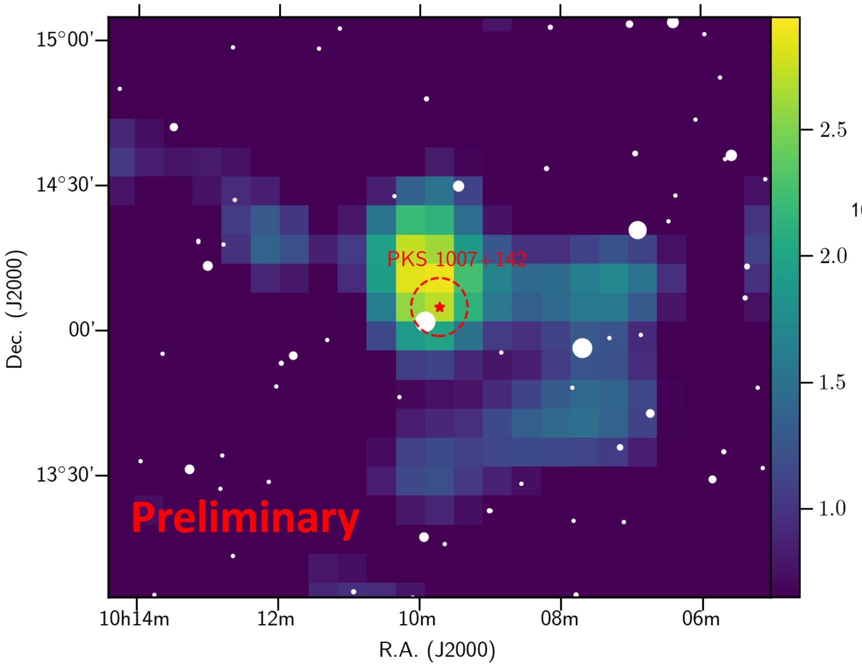

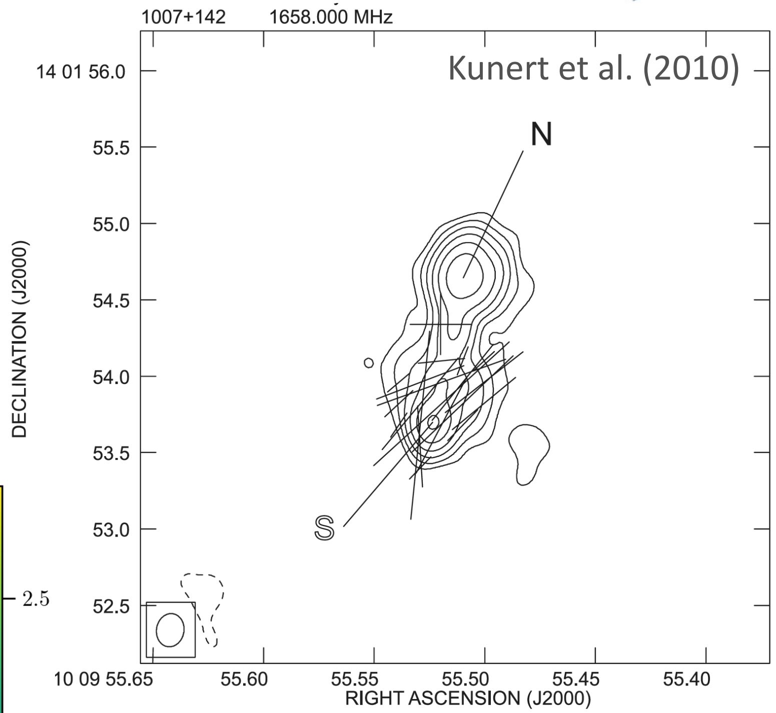

Fermi-LAT TS (in sigma unit).
White circles: radio sources (NVSS catalog). Dimensions are proportional to the flux (arbitrary scale).

The unusual quasar PKS B1413+135

Its classification has been debated for a long time (see also recent paper, Readhead et al. 2020), initially classified as BL Lac, then VLBA obs. showed: (1) a compact radio core, (2) a jet–like structure on a parsec scale, (3) and a counter–jet. The presence of a counter–jet disagrees with the blazar scenario. *The detection of a bright gamma-ray flare on August 2019* (see also ATel 13049) *supports the idea that the gamma-ray emission is beamed and produced by a relativistic jet at relatively small viewing angle.*

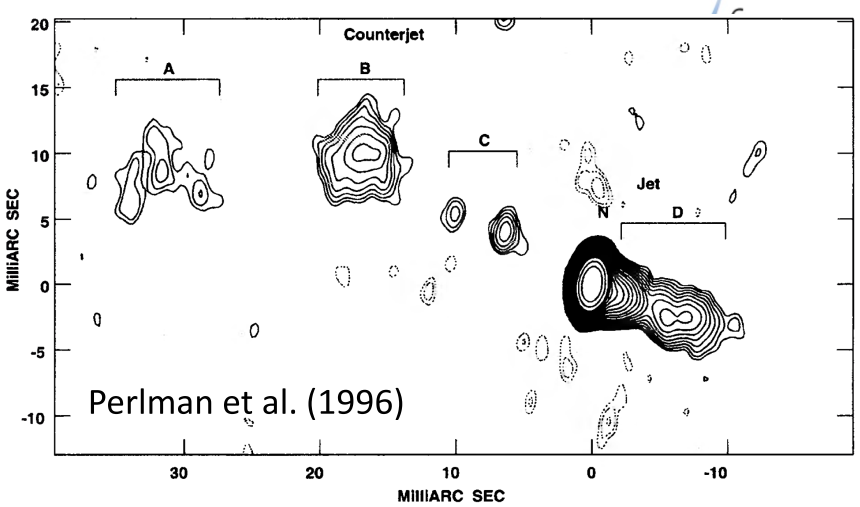

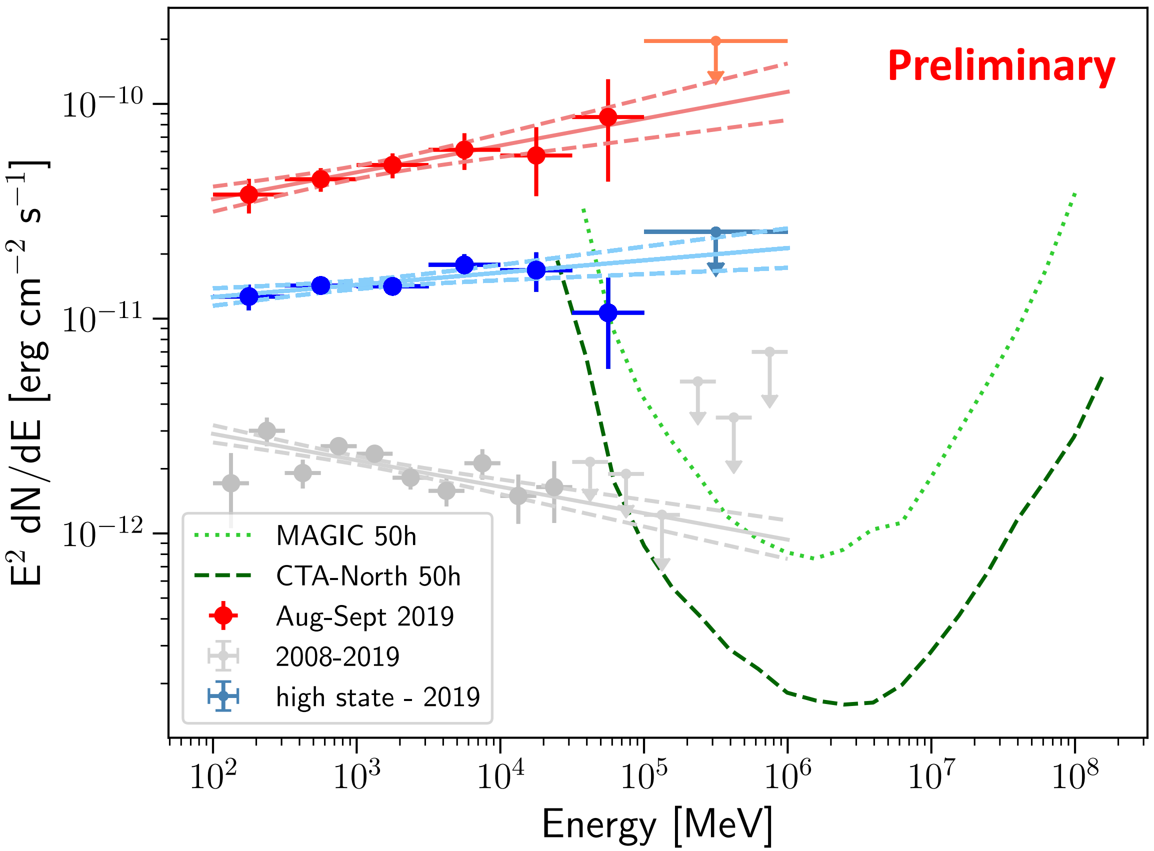

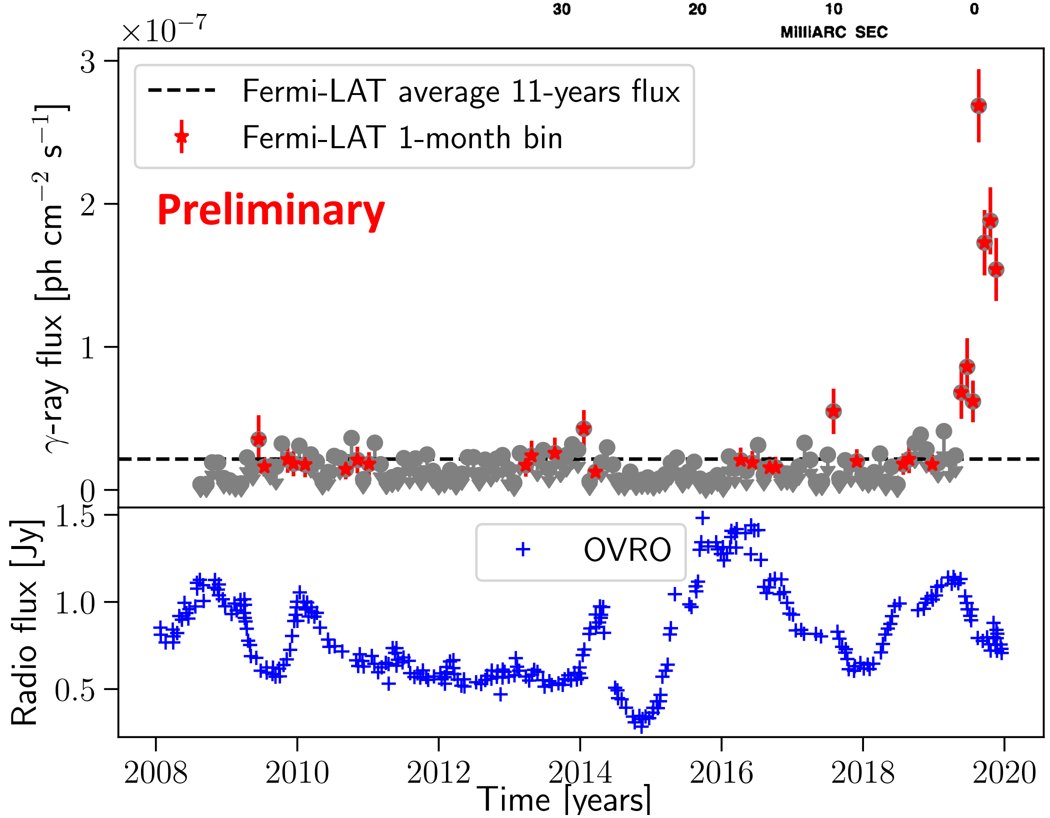

Gamma-ray luminosity and Fermi-LAT sensitivity

	Name	type	z	LS kpc	ν_p GHz	log $L_{5\,\mathrm{GHz}}$ W Hz^{-1}	TS	Flux$_\gamma$ 10^{-9} cm^{-2} s^{-1}	Γ	Lum$_\gamma$ 10^{44} erg s^{-1}
GALAXIES	0404+768	CSO/GPS	0.598	0.866	0.55	27.53	12	2.70±0.81	2.61±0.29	22.2
	1323+321	CSO/GPS	0.369	0.305	0.68	27.07	19	1.36±0.41	2.15±0.23	4.0
	3C346	LSO/CSS	0.162	22.056	<0.045	25.99	13	1.23±0.43	2.07±0.20	0.82
	1843+356	CSO/GPS	0.763	0.022	2	27.32	11	0.59±0.24	1.93±0.24	22.6
	J140051+521606	CSO/CSS	0.116	0.32	<0.15	24.36	17	0.12±0.05	1.64±0.32	0.20
	J083411.09+580321.4	CSO/CSS	0.093	0.0086	<0.4	24.13	15	3.53±0.96	2.66±0.20	0.30
	J092405.30+141021.4	CSO/CSS	0.136	0.74	<0.4	24.18	13	2.15±0.69	2.33±0.24	0.58
	J155235.38+441905.9	MSO/CSS	0.452	6.93	<0.4	25.56	17	0.78±0.26	2.07±0.19	6.0
QSO	3C147	MSO/CSS	0.545	4.454	0.231	27.92	22	6.89±1.51	2.69±0.16	47.120

Nine sources present a not negligible gamma-ray emission (TS>10, corresponding to a signif.$>3\sigma$), making them *promising gamma-ray candidates* for being possibly detected in the future.

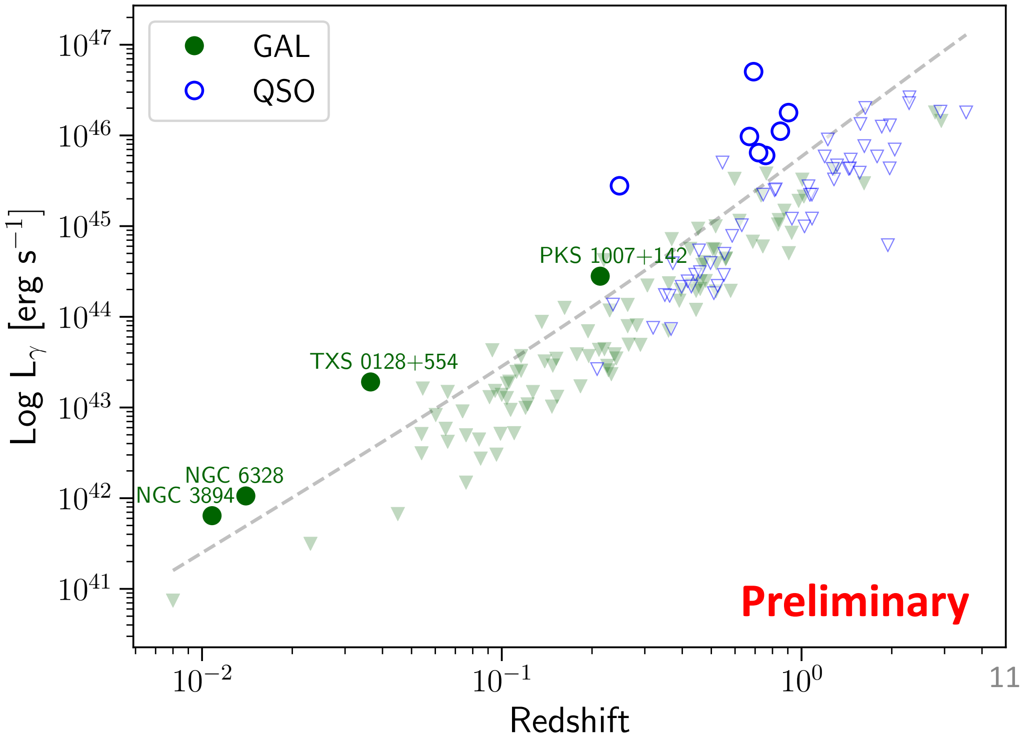

Stacking of young radio sources

We perform the first stacking analysis of the undetected young radio sources (galaxies and quasars). No significant emission has been detected. We repeated the stacking analysis for seven separate energy bands and we compared them with the averaged upper-limits of the undetected radio sources (grey band).

Select.	N	TS	F_γ^*	Γ
All	151	0.3	3.29	2.53
Galaxies	99	0.1	4.62	2.40
Quasars	52	0.2	10.09	2.64

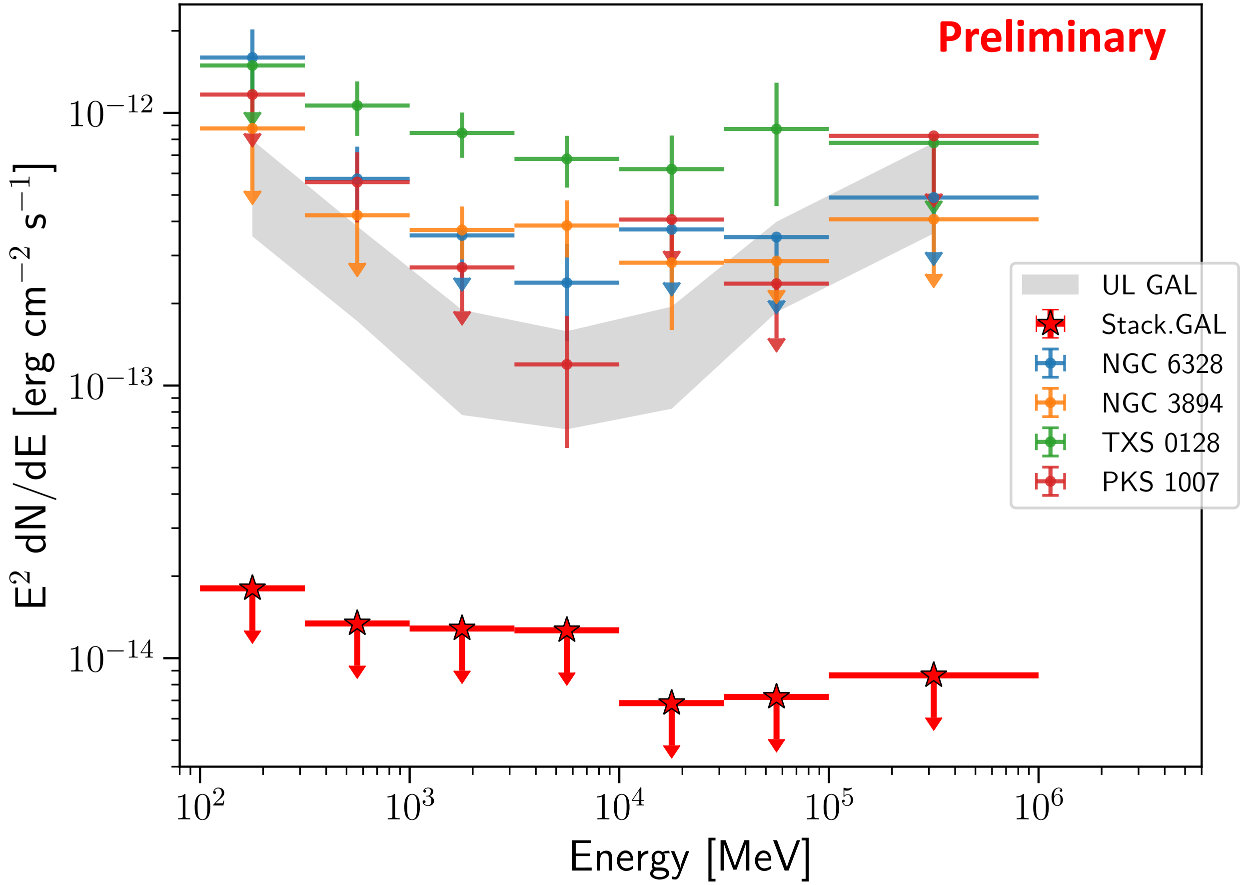

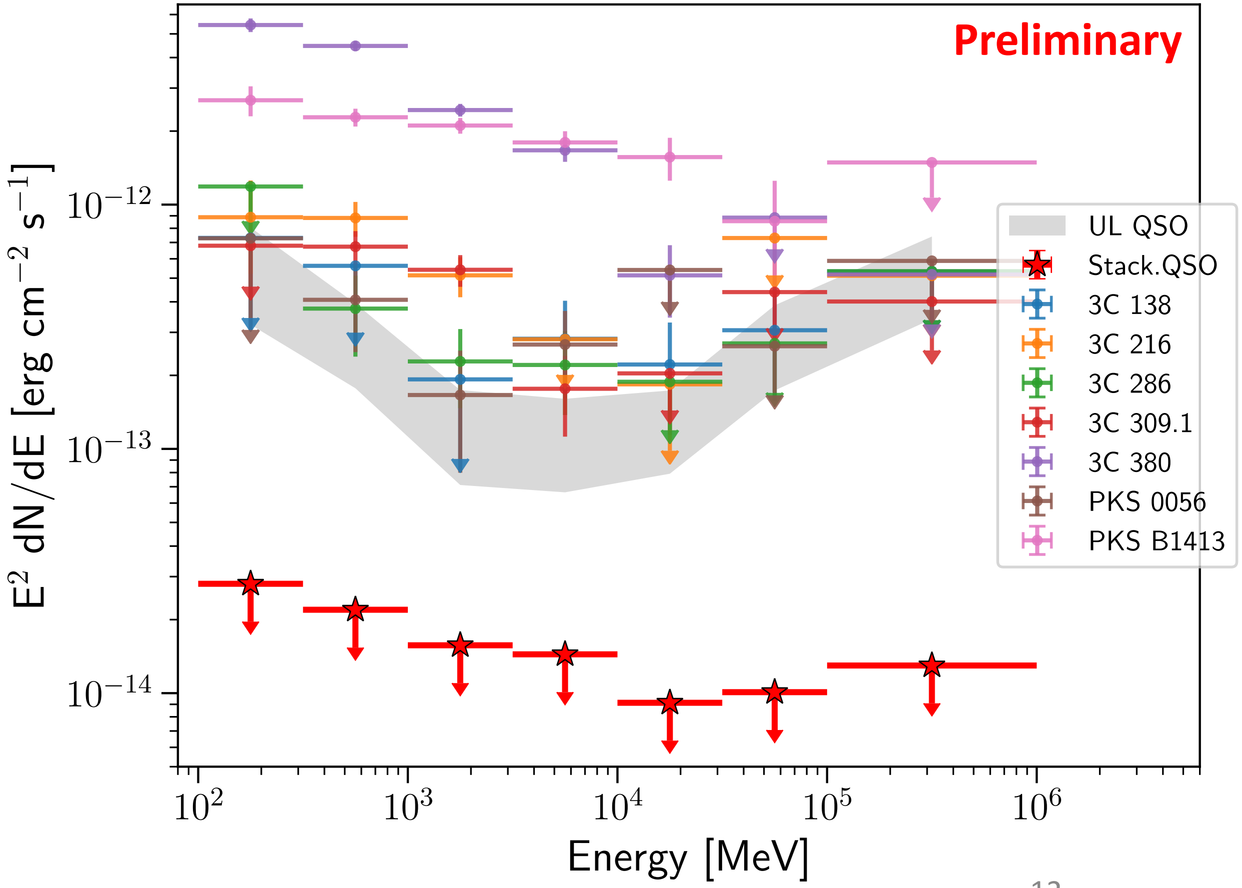

Stacking of selected subsamples

We performed the stacking analysis using different sub-samples defined by selections of the physical properties: nearby (z < 0.07, 0.15, 0.4, and 1) and compact (LS < 0.35, 0.5 and 1 kpc) sources, because they have been indicated as most promising candidates for gamma-ray emission in Stawarz et al. (2008). We found no detection. This allow us to say that <u>the parameters assumed in the model were too optimistic for the sources in our local Universe (d_L<300 Mpc, z<0.07).</u>

F*: UL in unit [10^{-11} ph cm^{-2} s^{-1}]

	Galaxies				Quasars			
Select.	N	TS	F^*_γ	Γ	N	TS	F^*_γ	Γ
LS<0.35	48	0.1	7.2	2.36	9	0.0	58.6	2.62
LS<0.5	52	0.1	9.4	2.38	13	0.1	46.1	2.58
LS<1	58	0.1	11.3	2.36	17	0.1	68.7	2.68
z<0.07	10	0.5	108	2.66	0	-	-	-
z<0.15	36	0.1	58.7	2.60	0	-	-	-
z<0.4	63	0.1	10.4	2.54	4	0.0	23.7	2.48
z<1	93	0.1	5.5	2.38	25	0.1	21.3	2.54
z<0.07 LS<0.15	8	0.8	172.9	2.78	0	-	-	-
z<0.15 LS<0.35	27	0.1	31.2	2.52	0	-	-	-
z<0.4 LS<0.5	39	0.1	15.4	2.50	1	0.0	297.5	2.76
O14	37	0.1	4.6	2.50	15	0.1	44.8	2.80

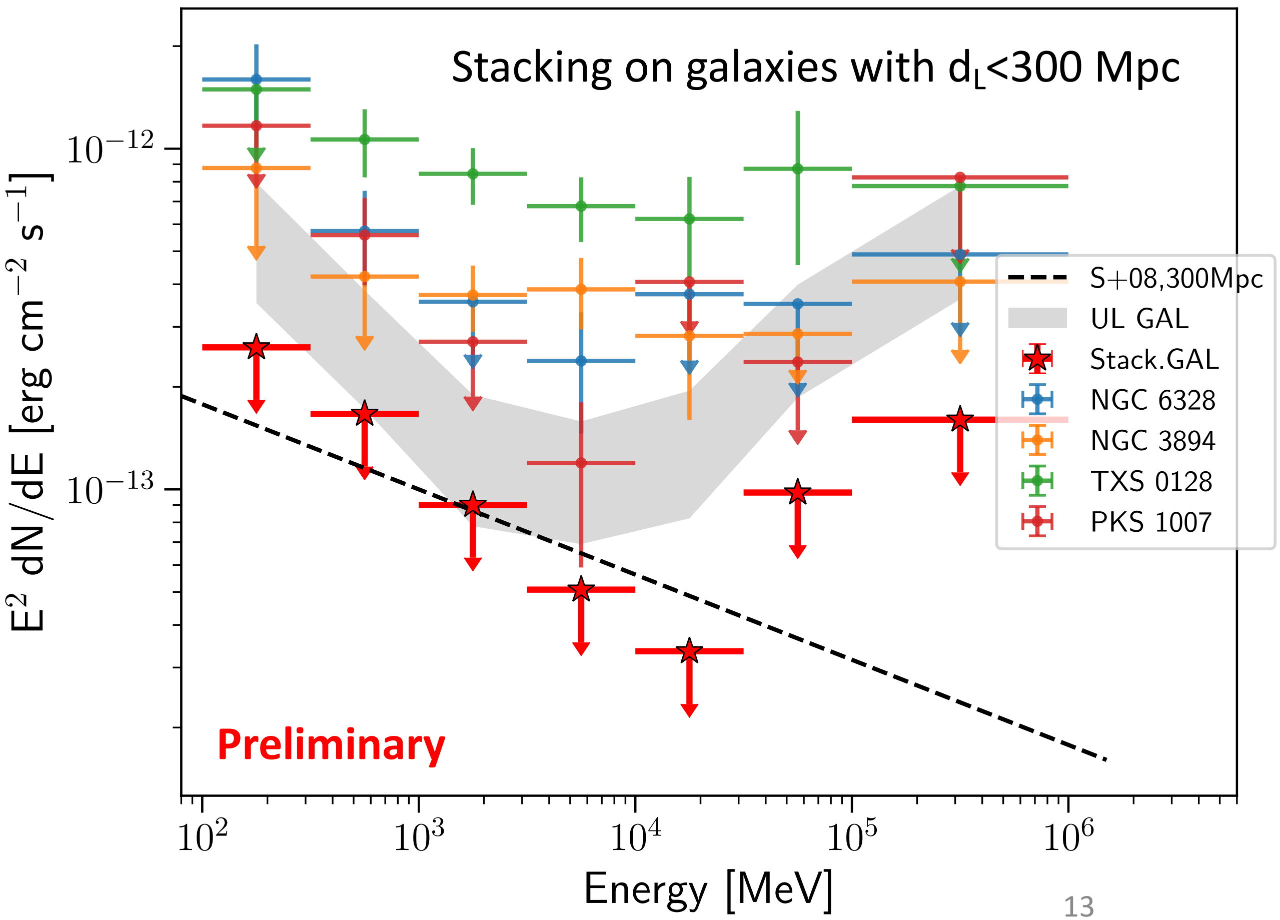

Comparison with gamma-ray expectations from galaxies

1. We repeated the stacking procedure by converting the gamma-ray flux UL into *constraints on the UV and jet luminosity*, using the information on LS and d_L of each individual source.

$$\frac{\epsilon L_\epsilon}{10^{42}\mathrm{erg/s}} \sim 2\frac{\eta_e}{\eta_B}\left(\frac{L_{\mathrm{jet}}}{10^{45}\mathrm{erg/s}}\right)^{0.5}\left(\frac{LS}{100\mathrm{pc}}\right)^{-1}\frac{L_{UV}}{10^{46}\mathrm{erg/s}}\left(\frac{\epsilon}{1\mathrm{Gev}}\right)^{-0.25}$$

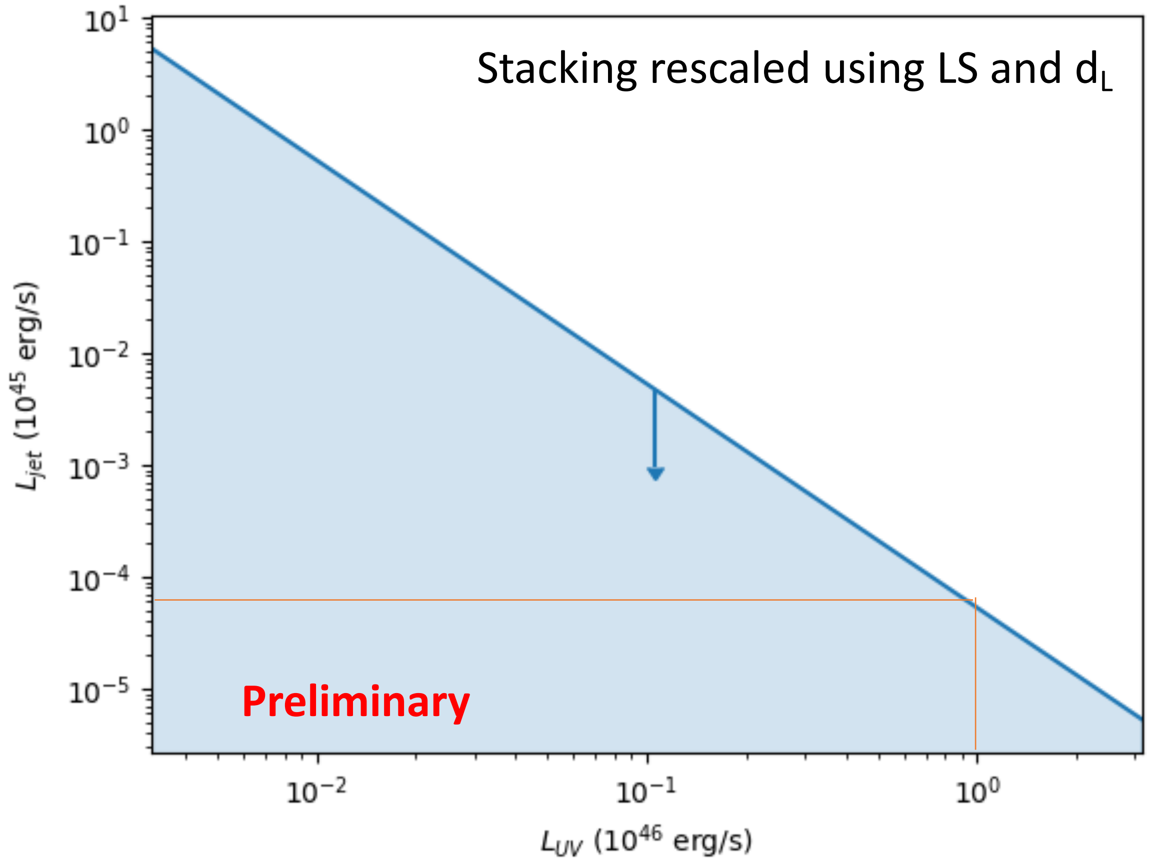

2. We estimated the number of sources needed to detect (reject) γ-ray emission assuming the prediction of Stawarz *et al. (2008)*, comparing the γ-ray expectations with the stacking analysis sensitivity (we performed the stacking analysis on 5 simulated dataset varying the simulated flux). *E.g.: at a d_L=300 (700) Mpc ≥2 (60) sources needed*

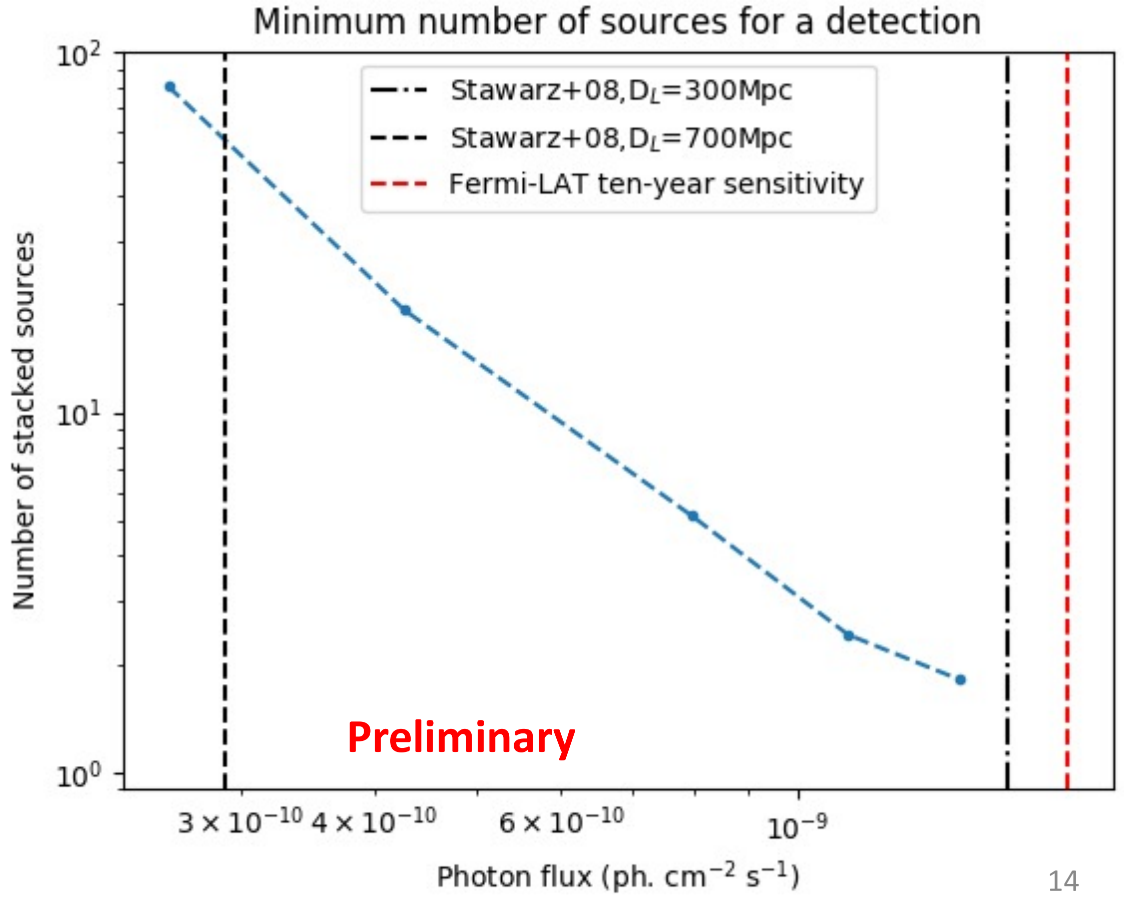

Origin of the gamma-ray emission

YRDG appear to share same γ-ray properties as other misaligned AGN in 4LAC

YQSO present a high gamma-ray luminosity, similar to FSRQ, suggesting that relativistic boosting is likely to play a role in their GeV detection.

Gamma rays in **YQSO** and **YRDG** may have a different origin: **jet** vs **radio lobes**.

PKS 1007+142 lies between the YQSOs and other YRDGs. While the other YRDGs are very nearby (z∼0.1) and compact (LS∼10 pc), it presents a more evolved structure (∼kpc) and it is located much further away (z∼0.2).

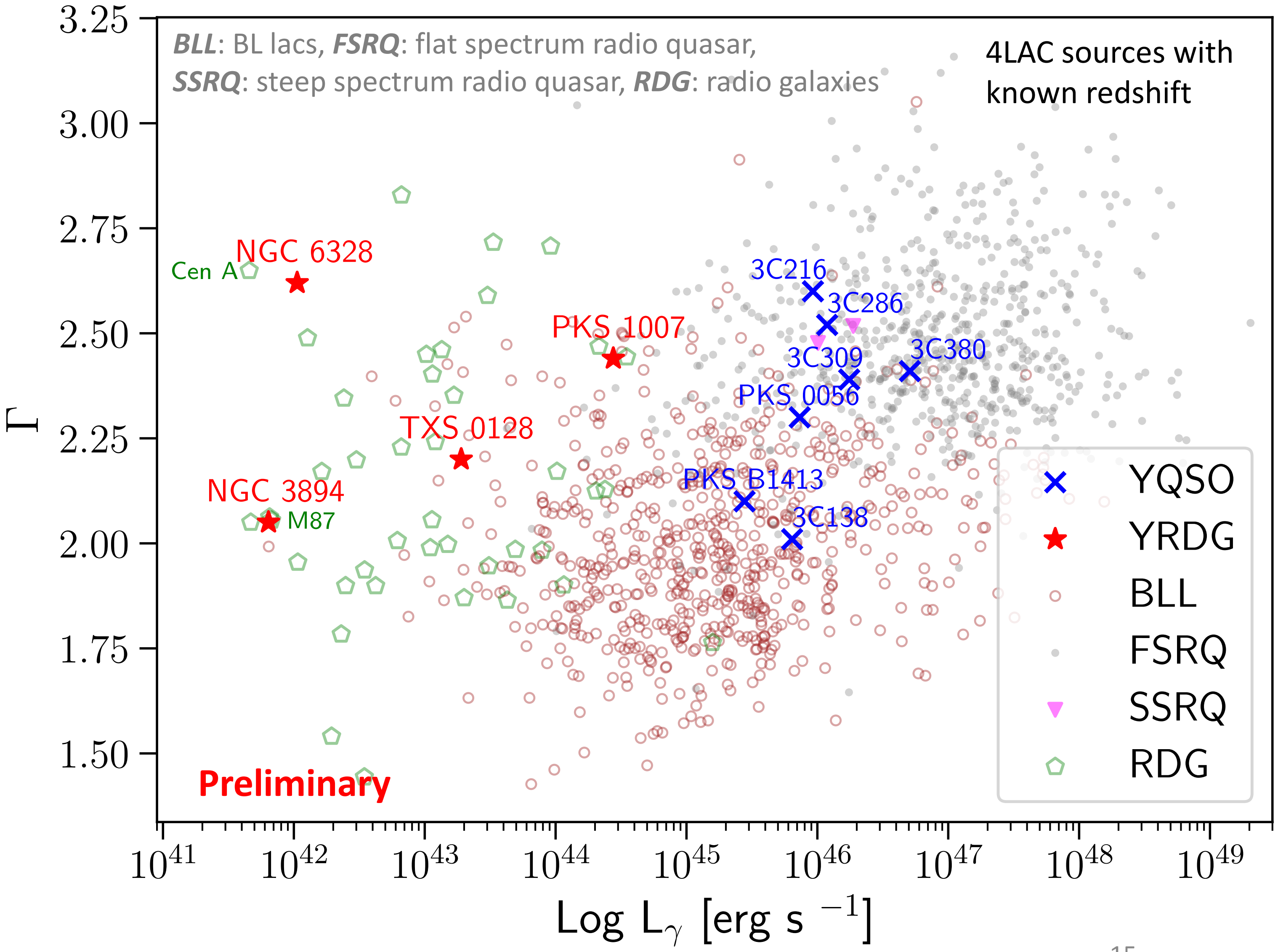

Conclusion

We perform the largest and deepest systematic search of gamma-ray emission from young radio galaxies and quasars using a sample of 162 sources and 11.3 years of Fermi-LAT data.

- we detect 11 young radio sources (4 galaxies and 7 quasars)
- we report the first LAT detection of the compact radio galaxy PKS 1007+128 (z=0.213)

We performed for the first time a stacking analysis on a sample of (undetected) young radio sources

- no significant emission found: resulting ULs are 10 times smaller than those on single sources.
- This allows us to say that the parameters assumed in the model of Stawarz+(08) were too optimistic for the sources in our local Universe (d_L=300 Mpc), while more sources are needed for a robust test of the model at larger distances. We constrain the UV and jet luminosity in Stawarz prediction, excluding gamma-ray emission from the brightest and most powerful sources.

Our results suggest that only the closest sources may be detected by Fermi-LAT, while considering objects at higher and higher redshift, boosting effects are necessary for their detection.

The paper has been submitted to MNRAS (stay tuned!!)

Thanks for your attention!

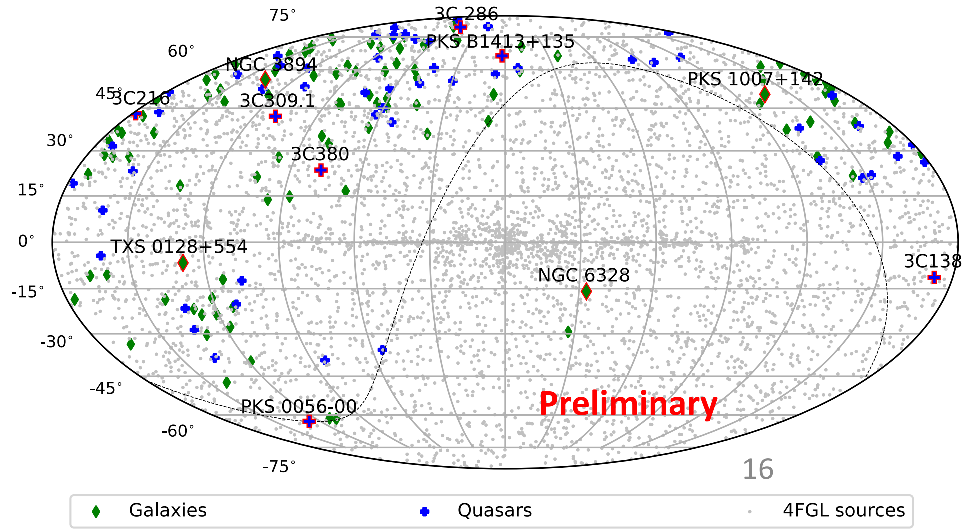

Backup slides

Gamma-ray expectations from young radio sources

Before the launch of Fermi-LAT [*Stawarz et. al. (2008)*]: *“The emission from the compact (<kpc) lobes in young radio sources is expected to extend up to GeV (or even TeV) energies.”*

*LS: Linear Size (100 pc)

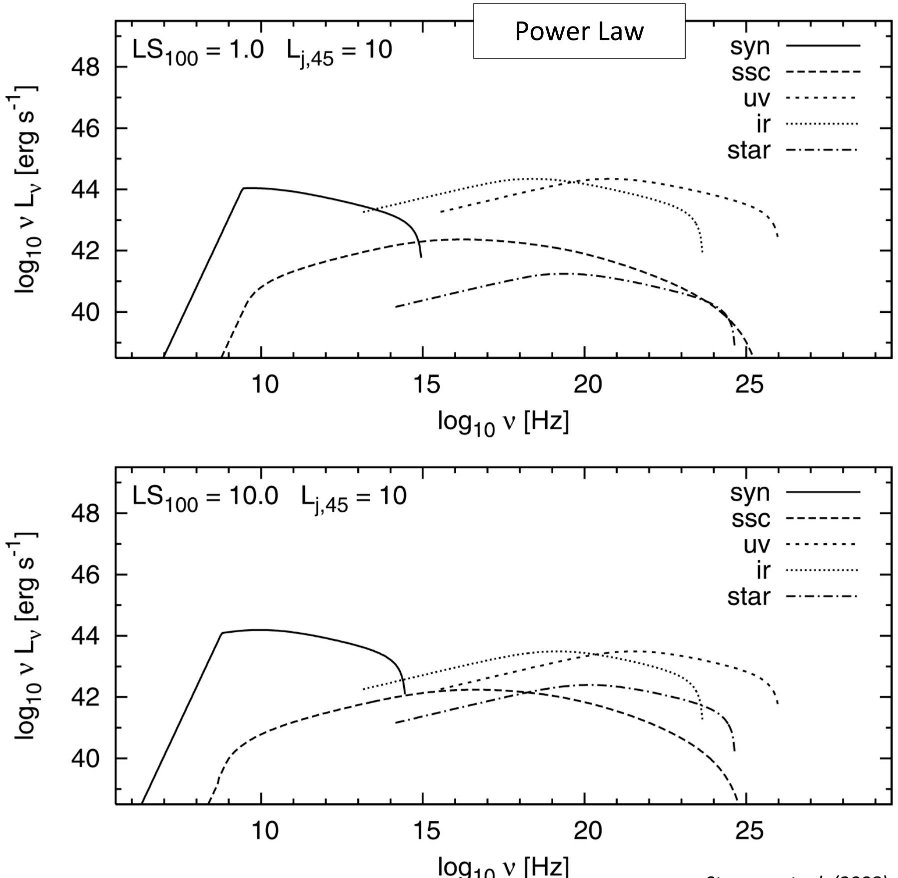

Stawarz et. al. (2008)

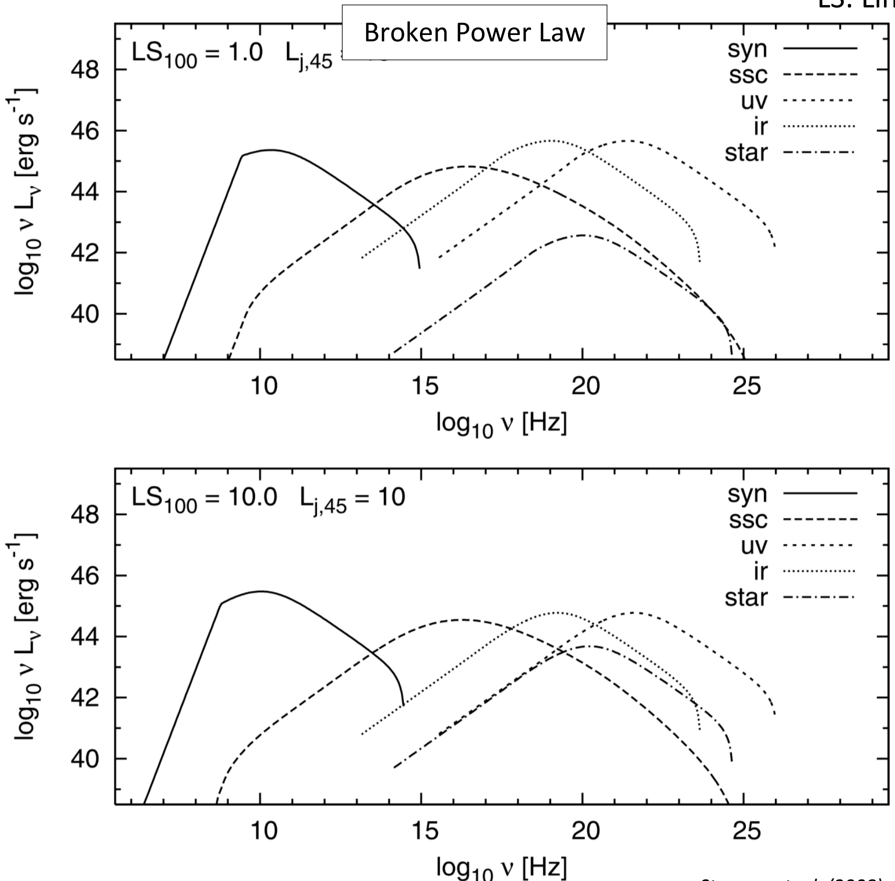

Stawarz et. al. (2008)

Stacking analysis: verification on simulated sources

We used the same pipeline implemented in the project about Omuamua (Ciprini et al., submitted).
To verify the robustness of our stacking method, we simulated 11 years of Pass 8 data for 100 sources at random positions, with same spectral characteristics (Γ=**2.25**, N_0=**3x10^{-14}** MeV^{-1} cm^{-2} s^{-1}) using a flux value below the LAT detection threshold. The stacking results Γ=2.26±0.13, N_0=(3.5±1.0)x10^{-14} MeV^{-1} cm^{-2} s^{-1}.

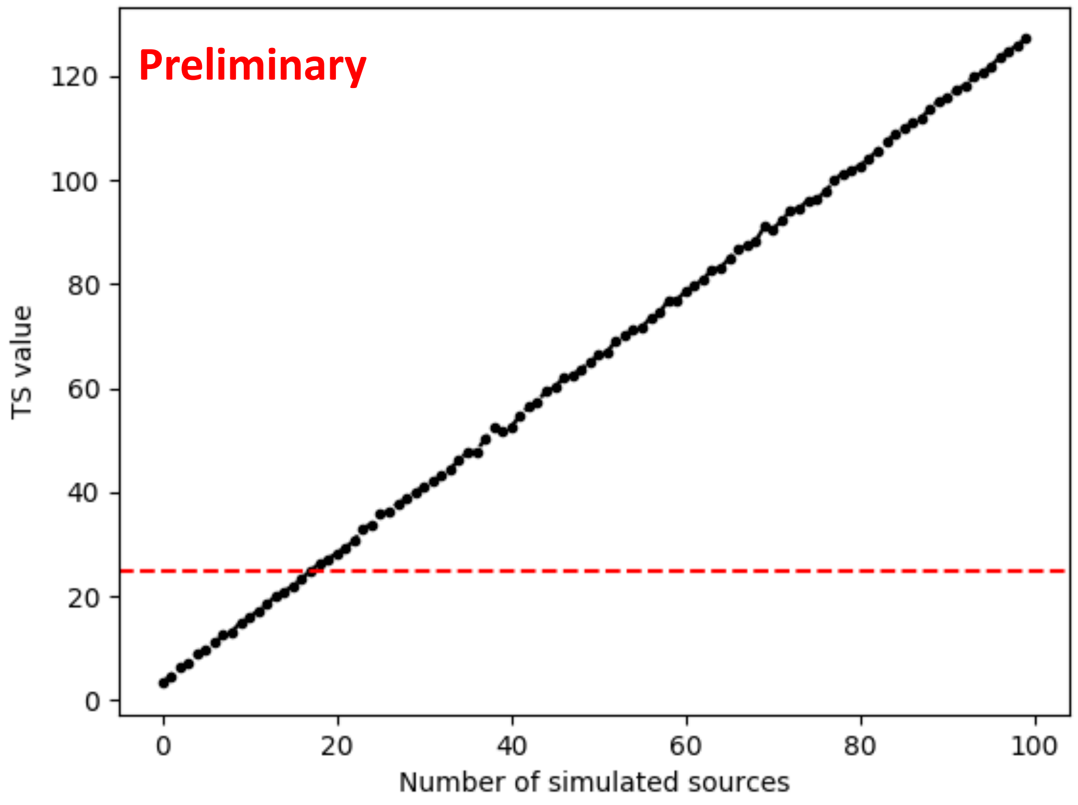

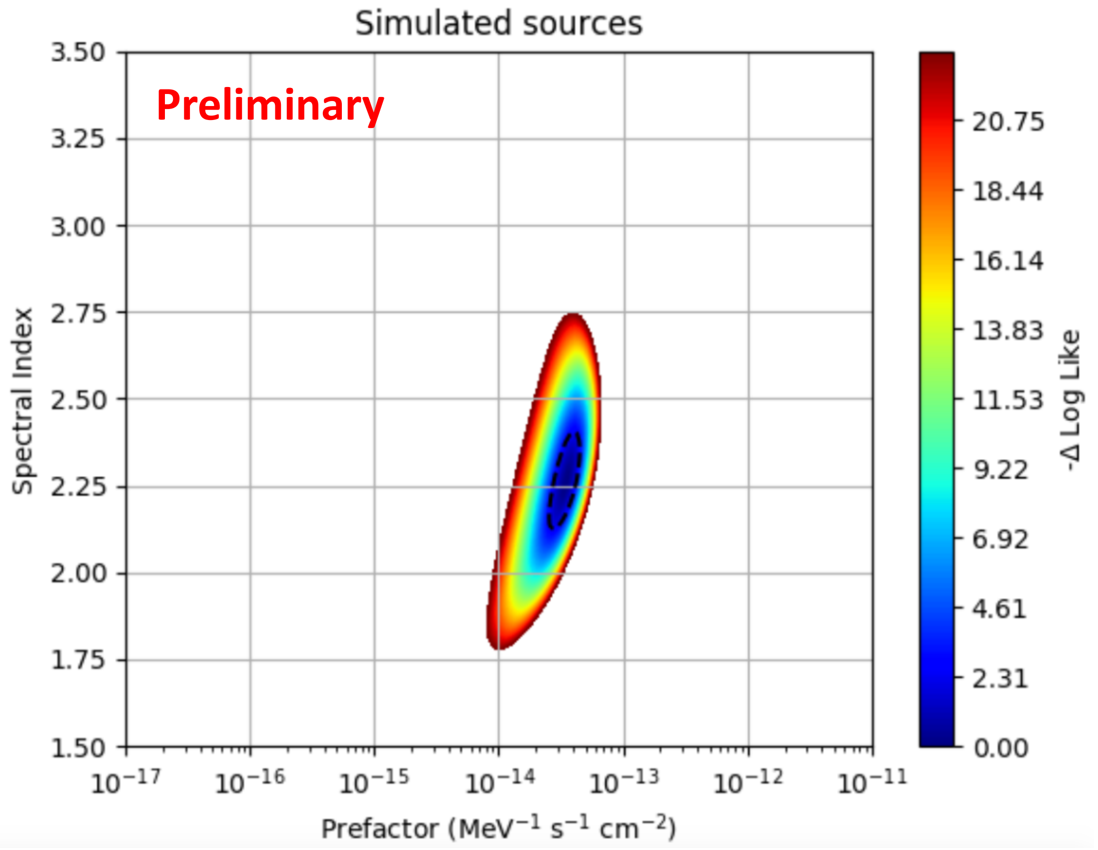

Stacking analysis: verification on background sources

To verify the quality of our results of the stacking analysis and see if they could be distinguished from simple background fluctuations, we performed the same analysis for background sources, using 100 random 'empty' positions.

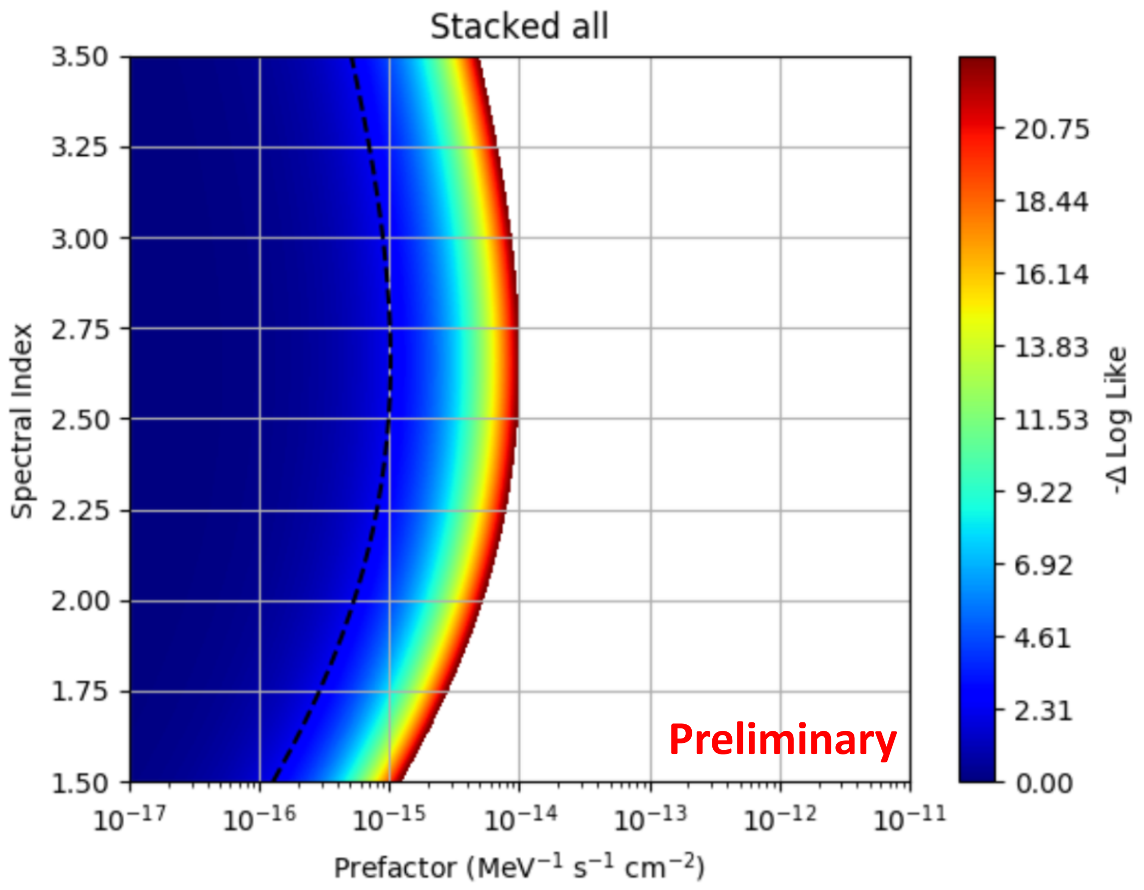

Stacking on young radio sources

We perform the first stacking analysis on the undetected young radio sources (galaxies and quasars). No significant emission has been detected for all the undetected sources.

Select.	N	TS	F_γ^*	Γ
All	151	0.3	3.29	2.53
Galaxies	99	0.1	4.62	2.40
Quasars	52	0.2	10.09	2.64

F*: UL in unit [10^{-11} ph cm^{-2} s^{-1}]

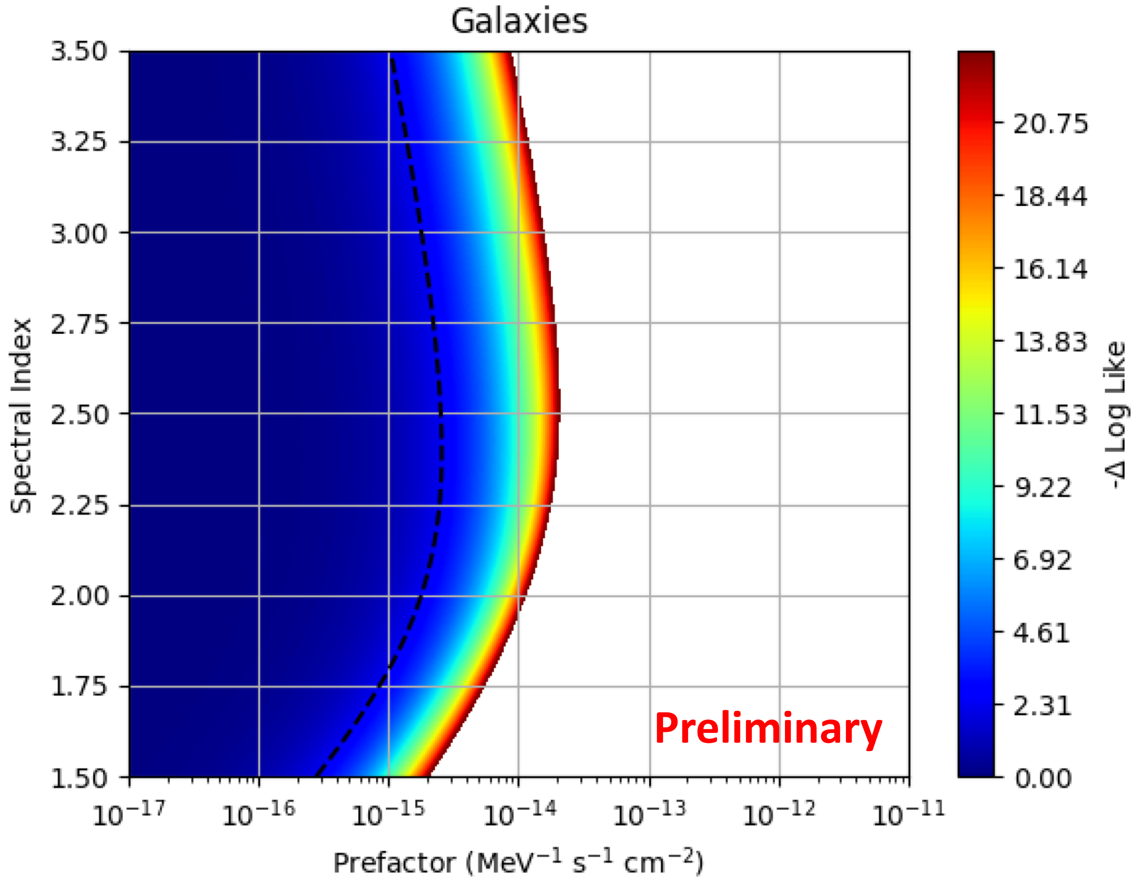

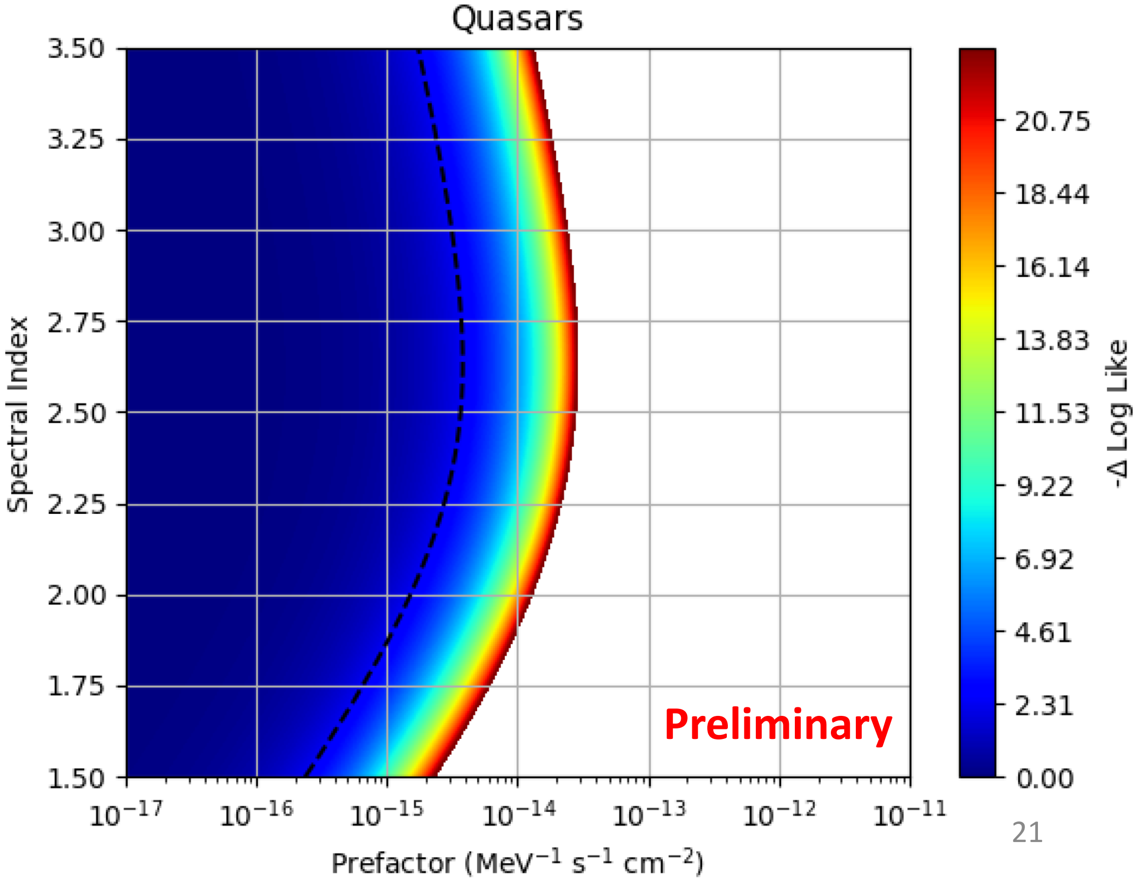

TXS 0128+554

TXS 0128+554 (z=0.0365) was previously classified as BCU. Recent multi-frequency radio VLBA study (Lister et al., 2020) measured the compact size (LS=12 pc), and misaligned nature (43 < ϑ < 59) classifying it as young radio galaxy with kinematic age of only 82±17 years.

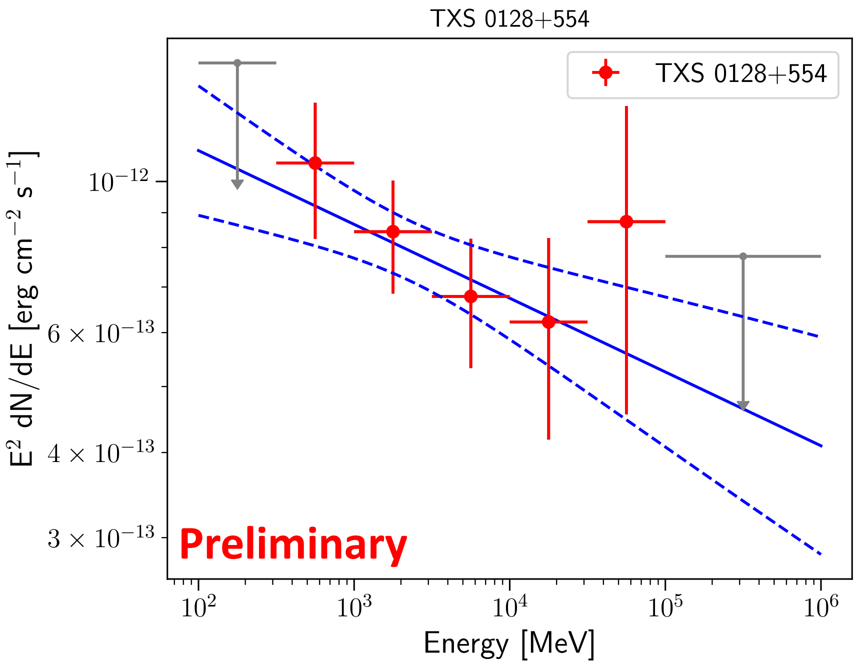

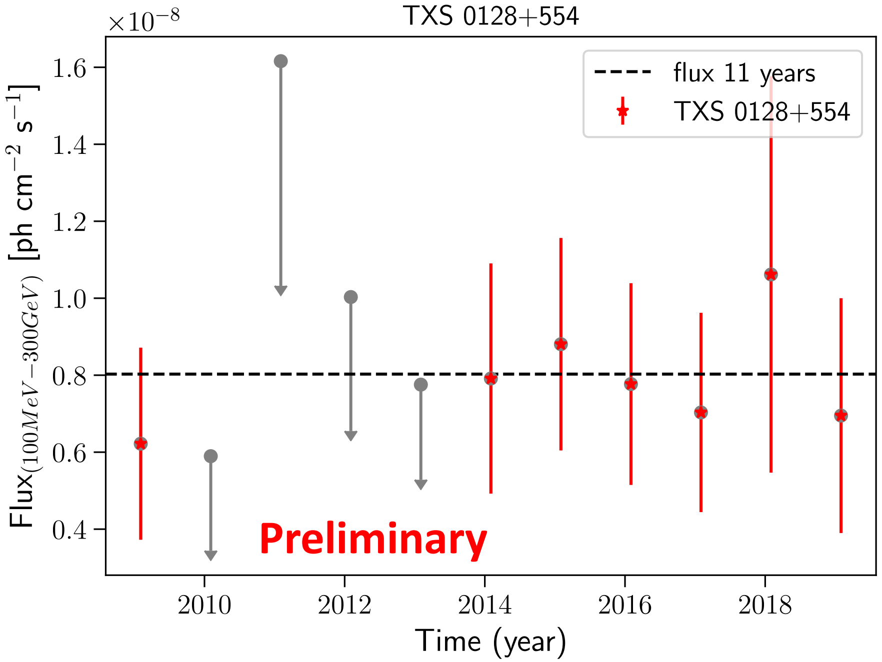

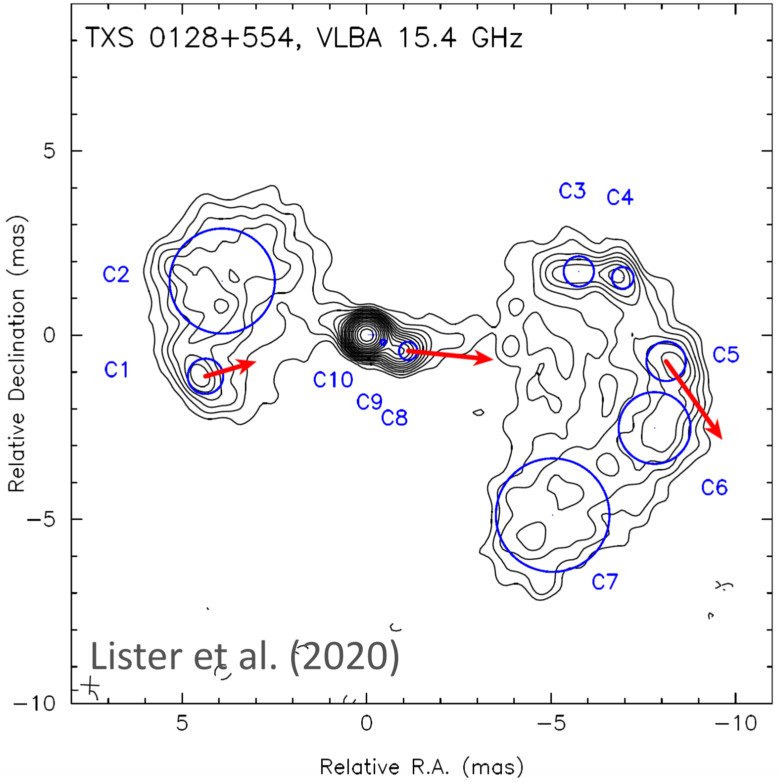

NGC 3894: a new young radio galaxy detected by Fermi-LAT

Principe et al. (2020)

(Fermi) We perform the Fermi-LAT analysis for the source using 11 yrs

- ❑ Observed faint γ-ray emission associated to NGC 3894
  (flat spetrum: $\Gamma = 1.99 \pm 0.10$)
- ❑ NGC 3894 appears to share same γ-ray properties as other misaligned AGN in 4LAC
- ❑ No γ-ray variability observed, as expected for CSO

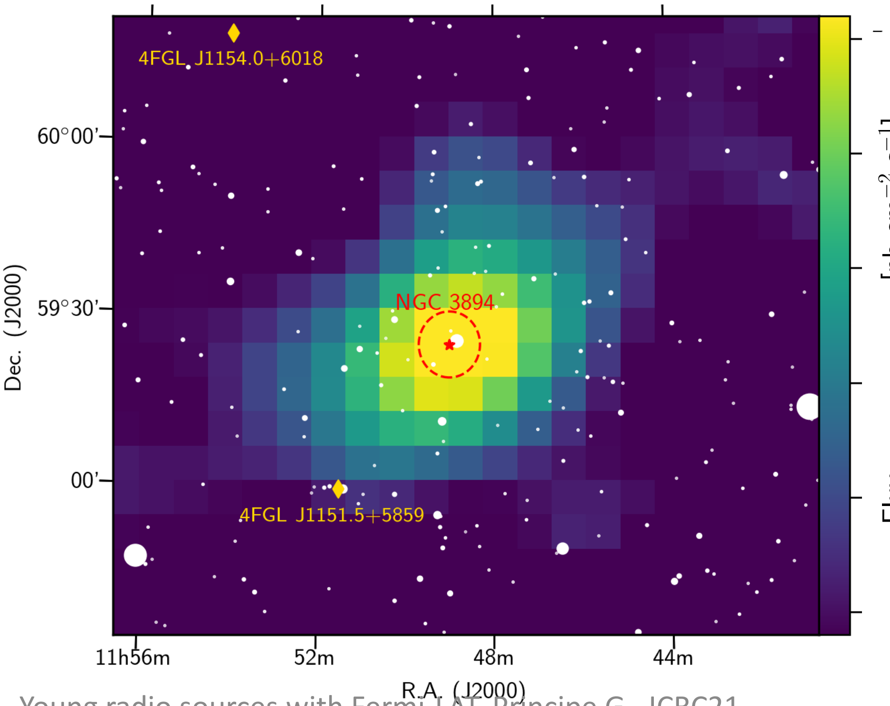

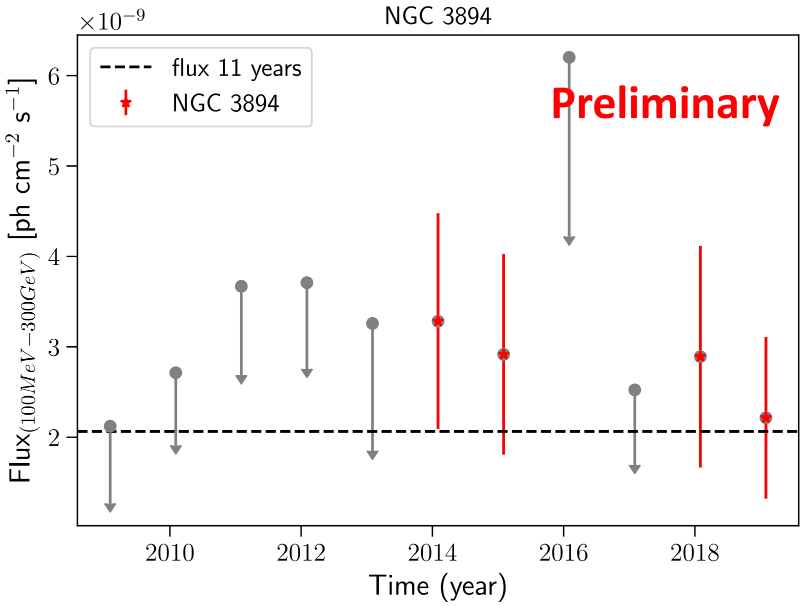

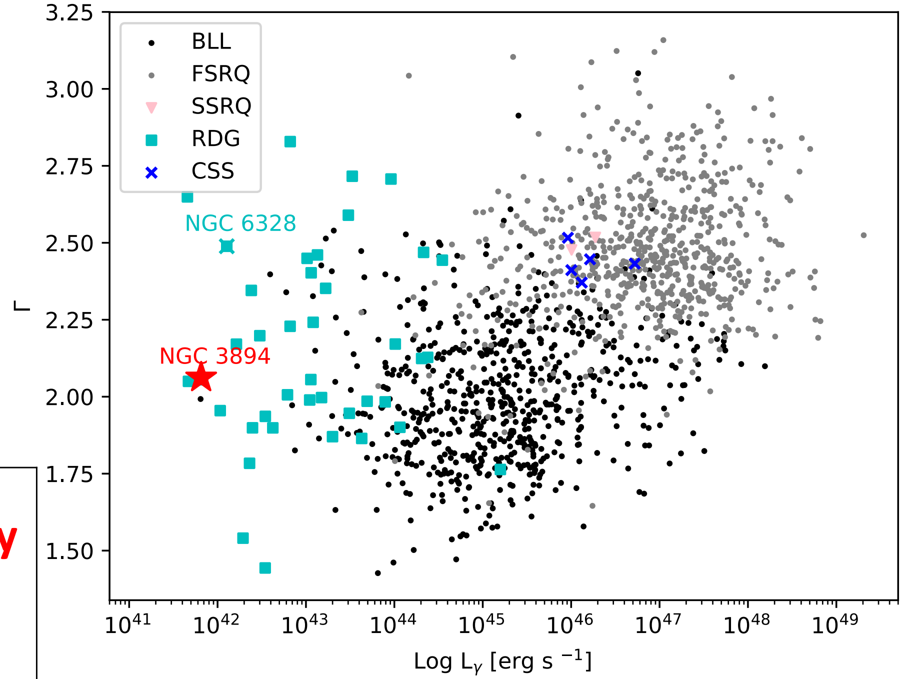

NGC 3894: a new young radio galaxy detected by Fermi-LAT

(VLBA) We have done a new radio analysis on archival VLBA data (1995-2017).
We established for NGC 3894 (z=0.01075) its nature of

- ❑ Young AGN --> estimated age: 58 $\pm$ 5 years (linear size ~ 4 pc)
- ❑ Misaligned AGN --> estimated viewing angle: 10°< θ< 21°, Doppler Factor δ~1.6

Principe et al. (2020)

eMERLIN proposal accepted (PI: PG)
Aimed at investigating the intermediate scale

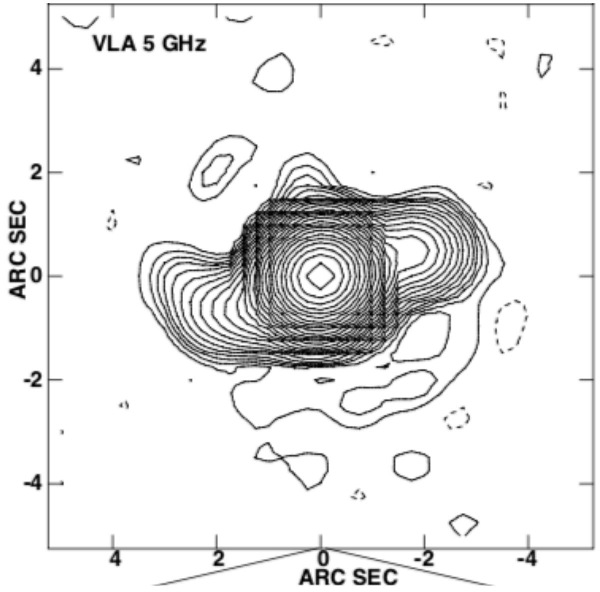

VLBA @8.4 GHz

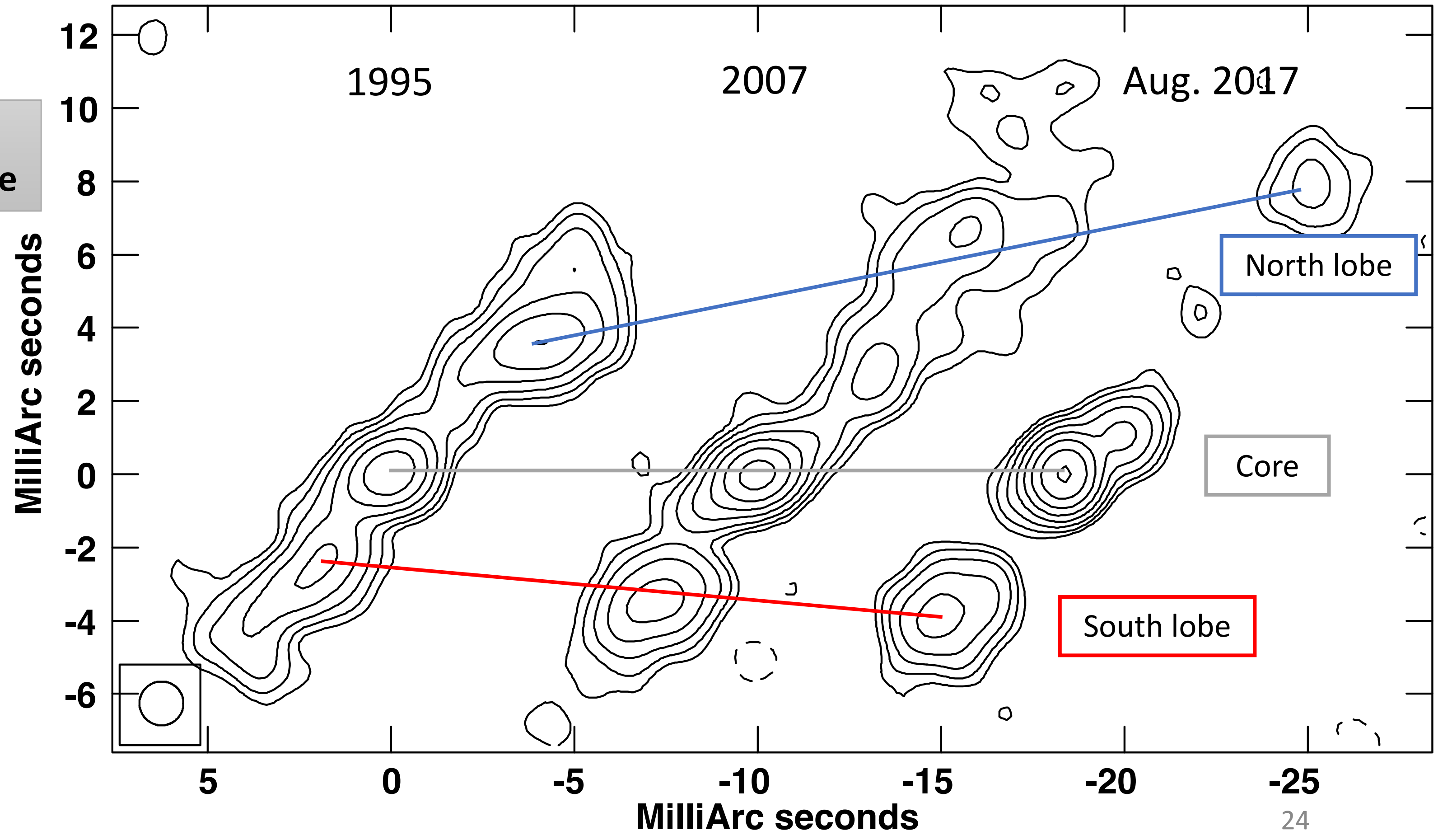

NGC 6328

NGC 6328 (PKS 1718–649)

Migliori et al. (2016) reported the discovery of gamma-ray emission by this young radio galaxy.

SED – PL: $\Gamma = 2.60 \pm 0.14$, F = $(5.3 \pm 1.5)\ 10^{-9}$ ph cm^{-2} s^{-1}, *TS= 36*

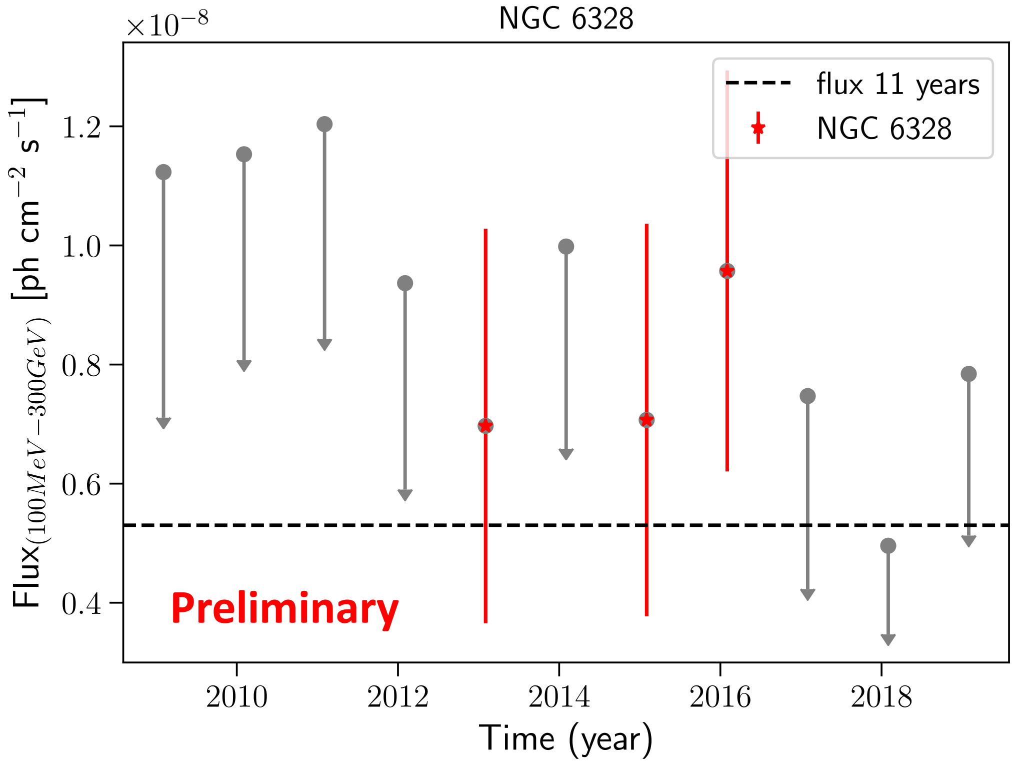

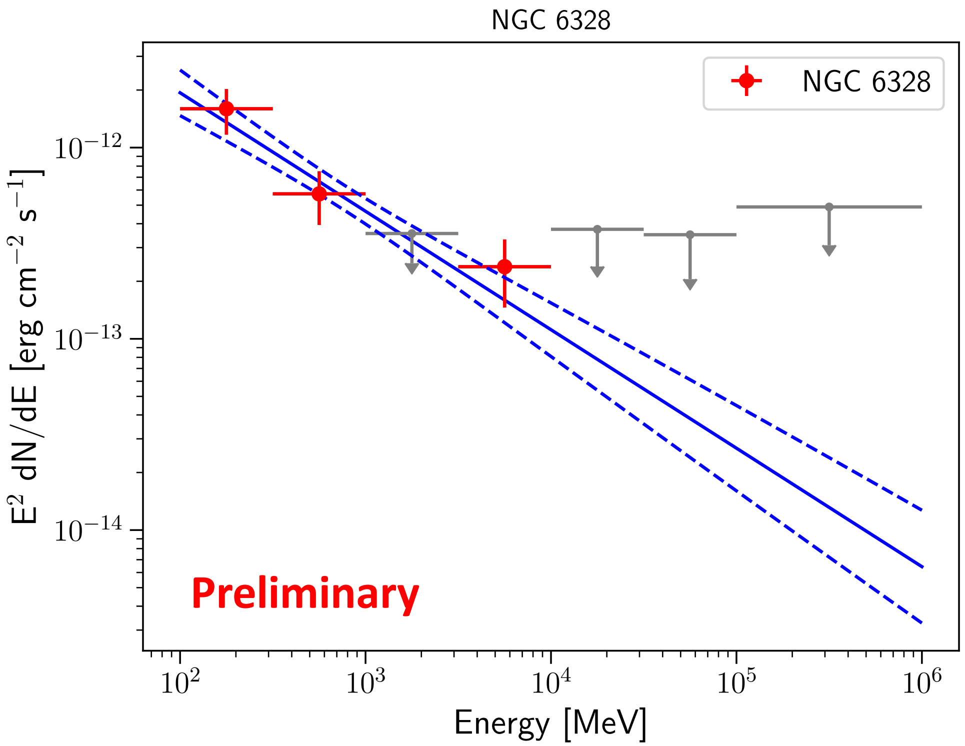

Another possible young radio galaxies observed by Fermi-LAT

PMN J1603–4904
Mueller et al. (2014)
Possible association of a 3FGL source to the young radio source PMN J1603-4904

This source however is not reported anymore in 4FGL as well as in 4FGL-DR2.

z	=	1.6
LLS (kpc)	=	0.125

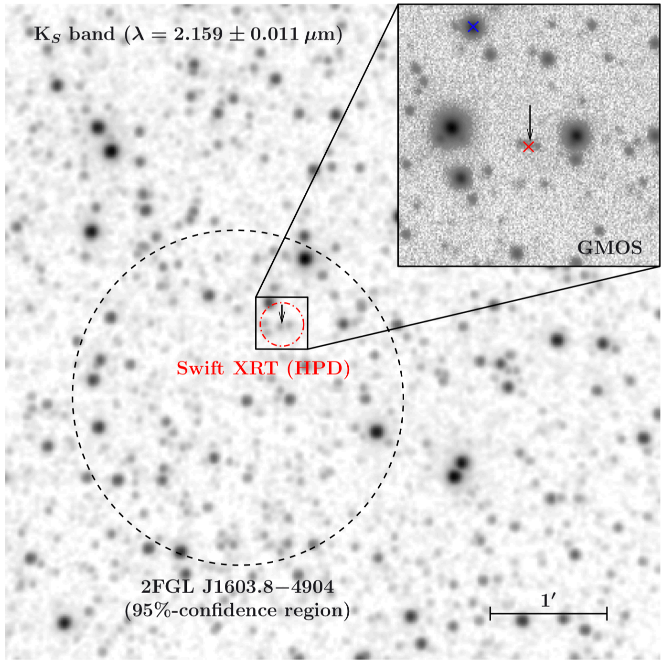

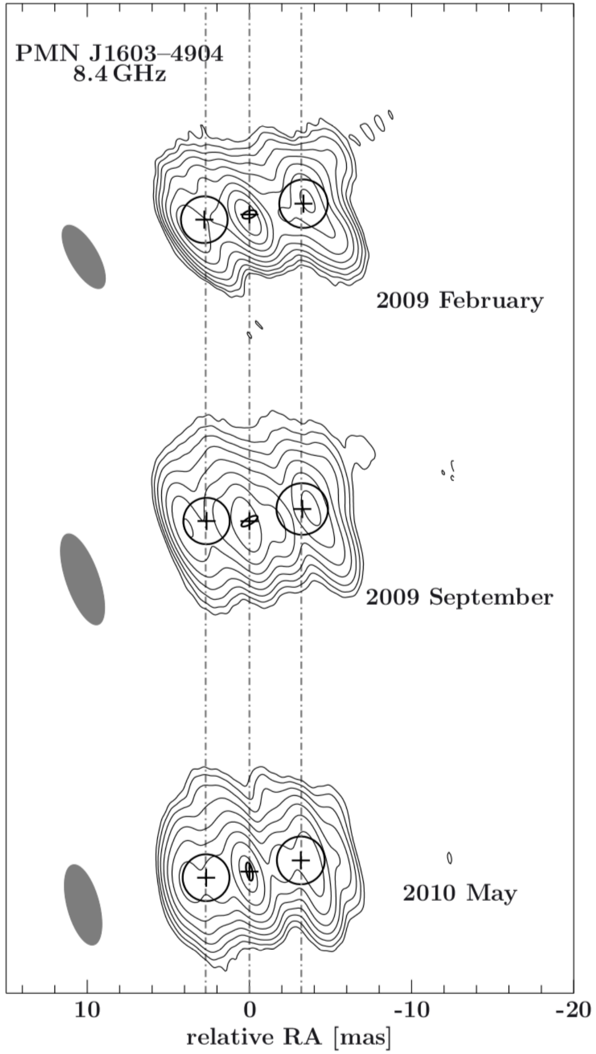

The case of the quasar 3C 138

The source had a strong gamma-ray flare in 2012, with only marginal detection until 2016.
(8 years, $\text{Gamma}_{4FGL} = 2.37 \pm 0.13$) (10 years, $\text{Gamma}_{4FGL\text{-}DR2} = 2.23 \pm 0.14$), (11.3 years, $\text{Gamma} = 1.95 \pm 0.14$).

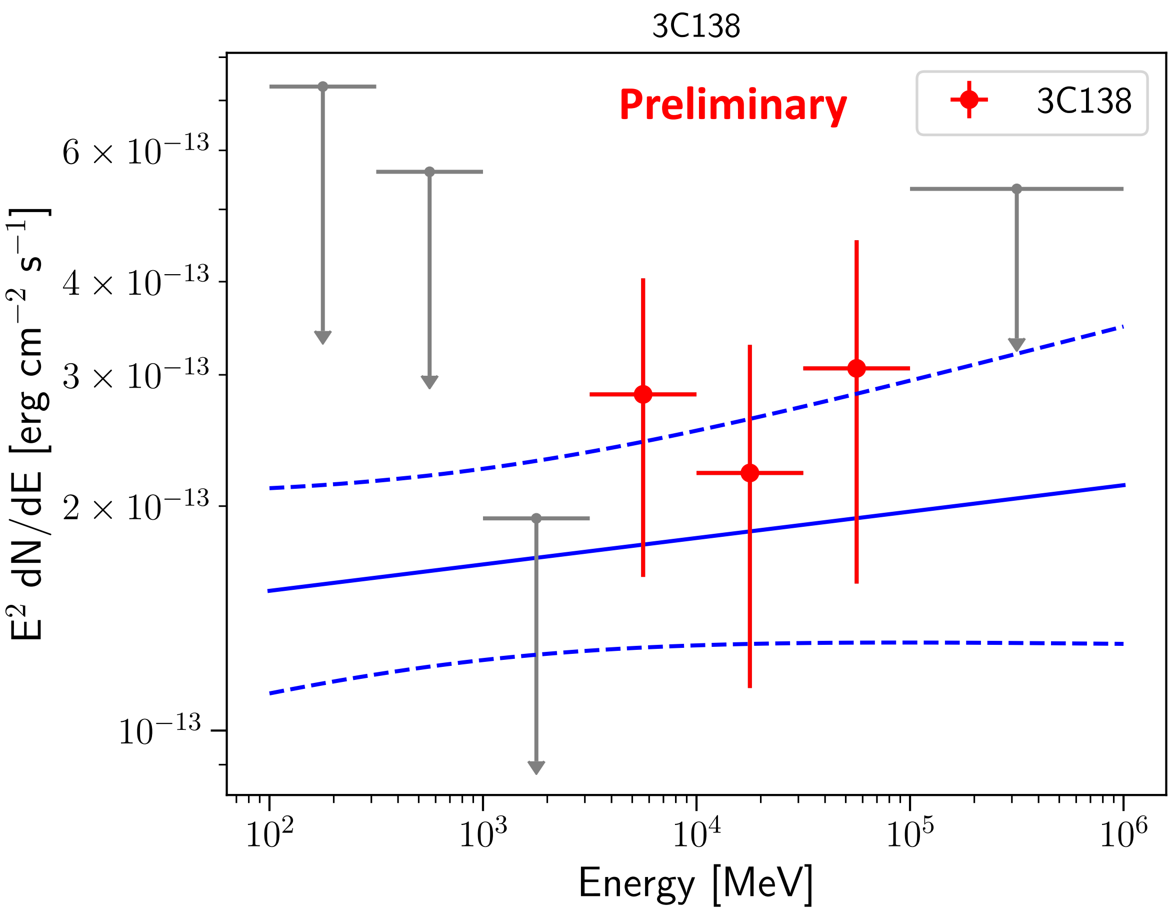

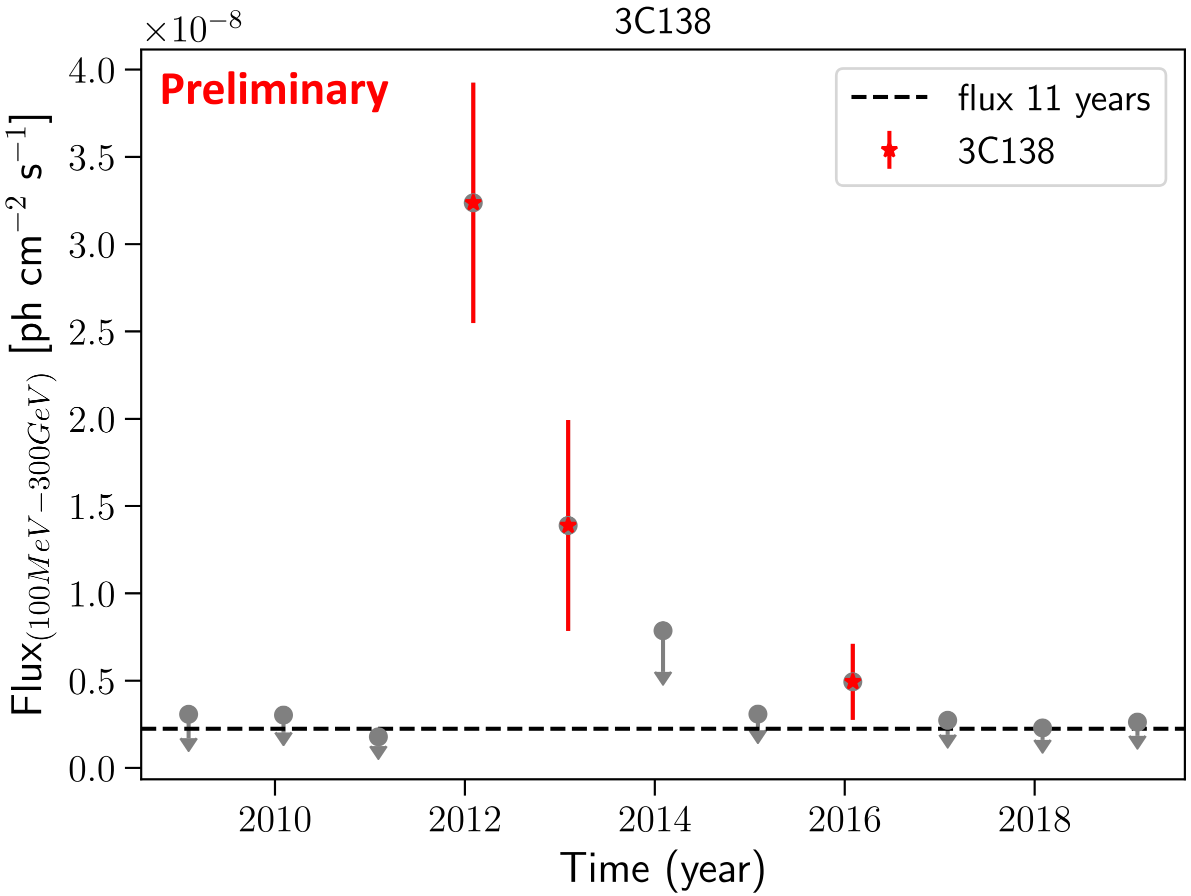

PKS 1007+142 lightcurve

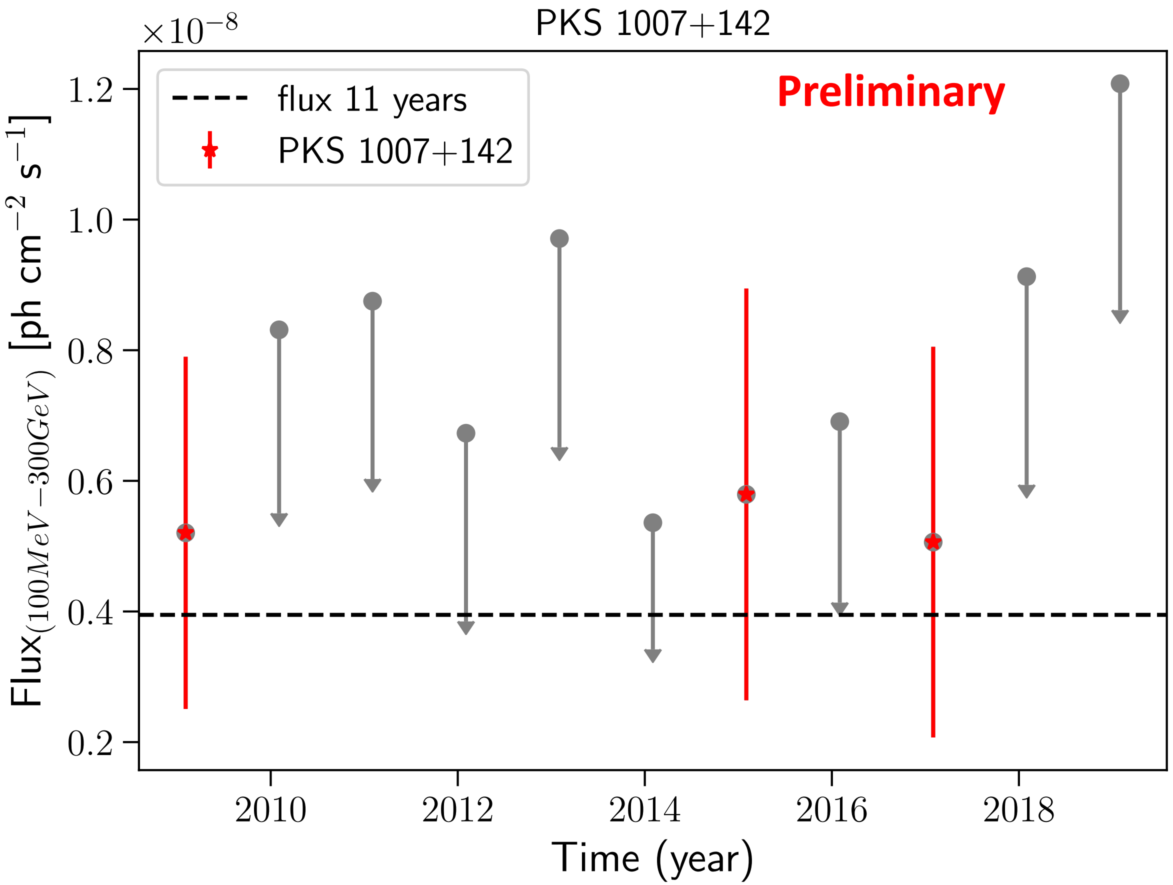

Undetected sources

In the appendix we provide a table with the Fermi-LAT results (UL) for all the sources contained in our sample

Table A.1. List of all young radio sources contained in our sample. We report in this table name, type (galaxy/quasar), redshift, projected linear size (LS) [kpc], radio turnover frequency (ν_p) [GHz], radio luminosity at 5 GHz [W Hz^{-1}], reference for radio information, gamma-ray significance (TS), gamma-ray flux (0.1–1000 GeV) in units of [10^{-9} ph cm^{-2} s^{-1}], power-law photon index (γ) and gamma-ray luminosity [10^{44} erg s^{-1}] of each detected source. We used a threshold of TS=10 for reporting upper limits on the gamma-ray flux and luminosity. References: dV09: de Vries et al. (2009), K20: Kosmaczewski et al. (2020), L20: Liao & Gu (2020), Li20: Lister et al. (2020), O04: Orienti et al. (2004) O08: Orienti & Dallacasa (2008), O14: Orienti & Dallacasa (2014), P20: Principe et al. (2020), R06: (Rossetti et al. 2006), W20: Wójtowicz et al. (2020), Z20: Zhang et al. (2020).

Name	type	z	LS kpc	ν_p GHz	log $L_{5\,GHz}$ W Hz^{-1}	Ref.	TS	Flux$_\gamma$ 10^{-9} cm^{-2} s^{-1}	Γ	Lum$_\gamma$ 10^{44} erg s^{-1}
OQ208	G	0.076	0.007	4.0	25.59	K20	0	<0.27	2.00	<0.050
J0111+3906	G	0.688	0.056	7.0	27.36	O14	0	<0.25	2.00	<6.763
J0650+6001	Q	0.455	0.04	8.0	26.93	O14	3	<0.55	2.00	<5.399
J1335+5844	G	0.58	0.105	8.8	26.94	O14	0	<0.11	2.00	<1.943